Minimally subtracted six-loop renormalization of $O(n)$-symmetric ϕ^4 theory and critical exponents

Mikhail V. Kompaniets*
Saint Petersburg State University, 7/9 Universitetskaya nab., Saint Petersburg 199034, Russia

Erik Panzer†
All Souls College, University of Oxford, OX1 4AL Oxford, United Kingdom

(Received 5 June 2017; published 31 August 2017)

We present the perturbative renormalization group functions of $O(n)$-symmetric ϕ^4 theory in $4-2\varepsilon$ dimensions to the sixth loop order in the minimal subtraction scheme. In addition, we estimate diagrams without subdivergences up to 11 loops and compare these results with the asymptotic behavior of the beta function. Furthermore we perform a resummation to obtain estimates for critical exponents in three and two dimensions.

DOI: 10.1103/PhysRevD.96.036016

I. INTRODUCTION

The field-theoretic renormalization group approach [1–3] has a long and successful history in the study of critical phenomena, going back to the famous ε expansion [4]. In particular, it predicts critical exponents of second-order phase transitions with high accuracy [5] when combined with resummation methods [6]. More specifically, one can extract approximate exponents for three-dimensional $O(n)$ universality classes from the renormalization group functions of ϕ^4 theory in $4-2\varepsilon$ dimensions.[1] Considerable effort has thus been invested in the calculation of the latter to increasingly high orders in perturbation theory.

After the results [8,9] for three and four loops, the computation [10–12] of the fifth order yielded highly accurate critical exponents [13]. The subsequent correction [14] of the perturbative result, which only very recently was confirmed by numeric methods [15], affected the resummed exponents only marginally [16].

For many years, the renormalization group method in three dimensions provided the most accurate theoretical predictions for critical exponents, consistent with the only slightly less precise results from the fifth-order ε expansion [16]. However, considerable progress of other techniques has by now produced a multitude of much more refined results. Among those, we like to point out the particularly astonishing performance of the conformal bootstrap program [17,18] and Monte Carlo methods [19,20], which reached unprecedented accuracy in some cases.

It was therefore overdue to improve on the ε expansion, which had been stuck at five loops for 25 years. Finally, the six-loop result for the field anomalous dimension was published in [21], and we provided the complete set of renormalization group functions for ϕ^4 theory ($n=1$) in [22]. These were obtained in a Feynman diagram computation, that became feasible through the automatization of new techniques [23–25] to calculate Feynman integrals, very briefly summarized in Sec. III.

Here, we present the six-loop renormalization group functions for arbitrary values of n, in the minimal subtraction scheme. The exact (and slightly unwieldy) expressions are given in Sec. IV, together with tables of numeric values for the most interesting cases $n \in \{0,1,2,3,4\}$. We then discuss numerous checks of our result and like to stress in particular the confirmation of the beta function and the field anomalous dimension, at $n=1$, by Schnetz [26]. Furthermore, we compare the coefficients of the beta function, supplemented by estimates up to 11 loops, with the expected asymptotic behavior. This analysis confirms the known fact that the convergence is rather slow in absolute terms, but it also shows that the qualitative trend is correct and we observe a striking pattern of zeros in the dependence on n, in agreement with the asymptotic prediction.

In Sec. V, we give the ε expansions for the critical exponents and recall the Borel resummation method with conformal mapping, which was employed to great effect in [9,13]. Since this basic idea can be implemented in many different ways and incorporates several arbitrary parameters, we include a rather detailed discussion of its characteristics. Our resummation algorithm is accurately defined in Sec. V C, followed by a discussion of how we estimate the errors.

Finally, our resummed results for the critical exponents in three and two dimensions are summarized and discussed

*m.kompaniets@spbu.ru
†erik.panzer@all-souls.ox.ac.uk

[1]Another approach renormalizes the theory directly in three dimensions [5,7].

in Secs. VI and VII. The reader only interested in these results will find them in Tables XI and XII. In short, we find increased accuracy (in comparison to the five-loop resummation) and good agreement with results from other methods. While the record precision for η and ν in the cases $n = 0$ and $n = 1$ from bootstrap and Monte Carlo methods is clearly out of reach, the ε expansion seems superior for the correction to scaling exponent ω and is on par for the Fisher exponent η when $n \geq 2$. Values for ν tend to be low in comparison with simulations in three dimensions and the theoretical predictions in two dimensions.

In our conclusion, Sec. VIII, we anticipate that the upcoming seven-loop renormalization [26] is very likely to result in estimates with smaller uncertainties, which will provide even stronger tests of the compatibility of different theoretical approaches.

We hope that our results will be useful for further analyses. In particular, it would be interesting to compare our critical exponents with other resummation methods applied to the six-loop series. Another application might be to probe the asymptotic behavior of the renormalization group functions, as in [27,28]. Also, the ε expansions and Z-factor contributions of individual diagrams should suffice to study other universality classes like the $O(n)$ model with cubic anisotropy [29,30] or even more complicated cases like [31,32].

Therefore we provide an extensive set of data with this article in Appendix A.

II. FIELD THEORY AND RENORMALIZATION

We consider the theory of n scalar fields $\phi = (\phi_1, \ldots, \phi_n)$ with an $O(n)$ symmetric interaction $\phi^4 := (\phi^2)^2 = (\phi_1^2 + \cdots + \phi_n^2)^2$. In $D = 4 - 2\varepsilon$ Euclidean dimensions, the corresponding renormalized Lagrangian is

$$\mathcal{L} = \frac{1}{2} m^2 Z_1 \phi^2 + \frac{1}{2} Z_2 (\partial\phi)^2 + \frac{16\pi^2}{4!} Z_4 g \mu^{2\varepsilon} \phi^4 \quad (1)$$

and contains an arbitrary mass scale μ, such that g stays dimensionless. The Z factors relate the renormalized field ϕ, mass m and coupling g to the bare field ϕ_0, bare mass m_0 and bare coupling g_0 via

$$Z_\phi = \frac{\phi_0}{\phi} = \sqrt{Z_2}, \qquad Z_{m^2} = \frac{m_0^2}{m^2} = \frac{Z_1}{Z_2}, \quad \text{and}$$
$$Z_g = \frac{g_0}{\mu^{2\varepsilon} g} = \frac{Z_4}{Z_2^2}. \quad (2)$$

In dimensional regularization [33] and minimal subtraction, these Z factors depend only on ε and g and admit expansions into formal Laurent series

$$Z_i = Z_i(g, \varepsilon) = 1 + \sum_{k=1}^{\infty} \frac{Z_{i,k}(g)}{\varepsilon^k}, \quad (3)$$

where each $Z_{i,k}(g)$ is a formal power series in the coupling g. The renormalization group (RG) functions can be read off from the residues (at $\varepsilon = 0$) of the Z factors [34,35]. In particular, the beta function can be computed as

$$\beta(g, \varepsilon) := \mu \frac{\partial g}{\partial \mu}\bigg|_{g_0} = -2\varepsilon \left(\frac{\partial \log(g Z_g)}{\partial g} \right)^{-1}$$
$$= -2\varepsilon g + 2g^2 \frac{\partial Z_{g,1}(g)}{\partial g}, \quad (4)$$

whereas the anomalous dimensions for the field and mass are given by

$$\gamma_i(g) := \mu \frac{\partial \log Z_i}{\partial \mu}\bigg|_{g_0, m_0, \phi_0} = \beta(g) \frac{\partial \log Z_i(g)}{\partial g}$$
$$= -2g \frac{\partial Z_{i,1}(g)}{\partial g} \quad \text{for } i = m^2, \phi. \quad (5)$$

These RG functions are formal power series in the coupling g. The first terms

$$\beta(g, \varepsilon) = -2\varepsilon g + \frac{n+8}{3} g^2 + \mathcal{O}(g^3)$$

show that, at least for small $\varepsilon > 0$, the beta function admits a nontrivial zero:

$$g_\star(\varepsilon) = \frac{6}{n+8} \varepsilon + \mathcal{O}(\varepsilon^2) \qquad \text{such that } \beta(g_\star(\varepsilon), \varepsilon) = 0. \quad (6)$$

This *critical coupling* is a formal power series in ε and determines a fixed point of the renormalization group flow. This fixed point is IR attractive, meaning that the *correction to scaling exponent*

$$\omega(\varepsilon) := \beta'(g_\star(\varepsilon), \varepsilon) = \frac{\partial}{\partial g}\bigg|_{g = g_\star(\varepsilon)} \beta(g, \varepsilon) = 2\varepsilon + \mathcal{O}(\varepsilon^2) \quad (7)$$

is positive. The anomalous dimensions at the critical point define the *critical exponents*

$$\eta(\varepsilon) := 2\gamma_\phi(g_\star(\varepsilon)) \quad \text{and} \quad \nu(\varepsilon) := [2 + \gamma_{m^2}(g_\star(\varepsilon))]^{-1}, \quad (8)$$

which we compute as formal power series in ε. According to the leading terms

$$\gamma_\phi = \frac{n+2}{36} g^2 + \mathcal{O}(g^3) \quad \text{and} \quad \gamma_{m^2} = -\frac{n+2}{3} g + \mathcal{O}(g^2), \quad (9)$$

the first terms of their ε expansions are

$$\eta(\varepsilon) = \frac{2(n+2)\varepsilon^2}{(n+8)^2} + \mathcal{O}(\varepsilon^3) \quad \text{and}$$
$$\nu(\varepsilon) = \frac{1}{2} + \frac{(n+2)\varepsilon}{2(n+8)} + \mathcal{O}(\varepsilon^2).$$

We note that there are more critical exponents, but those are related to η and ν via the following *scaling*[2]*relations* [1], which, for the purpose of this paper, we simply take as definitions of α, β, γ and δ:

$$\gamma = \nu(2-\eta), \qquad D\nu = 2-\alpha, \qquad \beta\delta = \beta+\gamma,$$
$$\text{and} \quad \alpha + 2\beta + \gamma = 2. \tag{10}$$

The critical exponents and the correction to scaling exponent ω are independent of the renormalization scheme and they conjecturally describe phase transitions of numerous physical systems in several universality classes. In Sec. V we describe how we resummed the ε expansions to arrive at the estimates for these quantities in $D = 3$ and $D = 2$ dimensions as presented in Secs. VI and VII.

III. CALCULATIONAL TECHNIQUES

We compute the Z factors (2) as the counterterms for the one-particle irreducible correlation functions Γ_N of $N = 2$ and $N = 4$ fields, by expanding them as Feynman diagrams. The ultraviolet (UV) subdivergences are subtracted with the Bogoliubov-Parasiuk $\mathcal{R}'$ operation [36,37], such that

$$Z_1 = 1 + \partial_{m^2}\mathcal{K}\mathcal{R}'\Gamma_2(p, m^2, g, \mu),$$
$$Z_2 = 1 + \partial_{p^2}\mathcal{K}\mathcal{R}'\Gamma_2(p, m^2, g, \mu), \quad \text{and}$$
$$Z_4 = 1 + \mathcal{K}\mathcal{R}'\Gamma_4(p, m^2, g, \mu)/g. \tag{11}$$

In the minimal subtraction (MS) scheme, the form (3) of the Z factors is obtained by projecting onto the pole part with respect to the regulator $\varepsilon = (4-D)/2$:

$$\mathcal{K}\left(\sum_n c_n \varepsilon^n\right) := \sum_{n<0} c_n \varepsilon^n. \tag{12}$$

We use standard techniques [1–3] to simplify the computation:

(i) Acting with $-\partial_{m^2}$ squares a propagator, which is equivalent to a four-point graph with two vanishing external momenta. This way, Z_1 can be expressed in terms of a subset of the graphs contributing to Z_4 (Sec. 11.7 in [1]).

(ii) Using infrared rearrangement (IRR) [38,39], we can set all internal masses to zero and nullify some external momenta such that only massless propagators remain to be computed.

These express all Z factors in terms of p integrals (massless propagators) without infrared divergences, and our task is thus reduced to the computation of the ε expansion of these integrals. The number of ϕ^4 Feynman graphs contributing to Γ_2 and Γ_4 is summarized in Table I.[3] A few of them are primitive (free of subdivergences) and those were computed, up to ≤ 6 loops, already long ago in [42].[4] In fact, the partial results [43,47] at higher loop orders have recently been augmented significantly, including in particular the complete set of primitive ϕ^4 Feynman integrals with seven loops [48].

TABLE I. The number of (isomorphism classes of) one-particle irreducible ϕ^4 Feynman graphs, excluding graphs with tadpoles (as those vanish in massless DimReg). We include the column for seven loops just to illustrate the growth in complexity.

Loops	1	2	3	4	5	6	7
Two-point graphs (Γ_2)	0	1	1	4	11	50	209
Four-point graphs (Γ_4)	1	2	8	26	124	627	3794
Primitive four-point graphs (Γ_4)	1	0	1	1	3	10	44

In order to calculate the missing integrals with (UV) subdivergences, which was the main technical challenge, we construct auxiliary counterterms using the $\mathcal{R}'$ operation of the Bogoliubov-Parasiuk-Hepp-Zimmermann (BPHZ)-like *one-scale scheme* introduced in [25]. The resulting linear combinations of integrals are convergent in $D = 4$ dimensions and can thus be computed exactly, term by term after expanding in ε, with the program HyperInt [24] based on the algorithm proposed in [23].

We gave a detailed account of this new method in [22]. The entire computation is automated with programs written in Maple™ and Python, using the GraphState/Graphine library to manipulate Feynman graphs [49,50], which will be published separately.[5]

The only addition to be made to the exposition in [22] is that each Feynman graph G is now not only weighted with the usual combinatorial symmetry factor $1/|\mathrm{Aut}(G)|$, but also with an additional $O(n)$-*group factor* $\mathcal{C}_G$ which is a polynomial in n. It equals the number of ways one can assign a component $1 \leq i_e \leq n$ of the field ϕ to each of the edges e of the graph, in such a way that at each vertex v, the flavors of the four edges $v^{[1]}, \ldots, v^{[4]}$ meeting at v can be

[2]Relations that explicitly involve the dimension D are often distinguished and called *hyperscaling relations*. For simplicity, we will refer to all of (10) just as *scaling relations*.

[3]The ϕ^4 graphs with ≤ 6 loops were already enumerated and tabulated in [40]. Asymptotically, the number of graphs grows factorially with the number of loops and precise higher-order expansions were recently presented in [41].

[4]Some of the results in [42] in terms of zeta values were based on numeric techniques, and one value in particular was only later identified in [43] as the double zeta value (17). Analytic proofs of these six-loop periods were later given in [44–46].

[5]Maple is a trademark of Waterloo Maple Inc.

TABLE II. Numerical values for the six-loop field anomalous dimension.

n	$\gamma_\phi^{\mathrm{MS}}(g)$
0	$0.05556g^2 - 0.03704g^3 + 0.1929g^4 - 1.006g^5 + 7.095g^6 + \mathcal{O}(g^7)$
1	$0.08333g^2 - 0.06250g^3 + 0.3385g^4 - 1.926g^5 + 14.38g^6 + \mathcal{O}(g^7)$
2	$0.11111g^2 - 0.09259g^3 + 0.5093g^4 - 3.148g^5 + 24.71g^6 + \mathcal{O}(g^7)$
3	$0.13889g^2 - 0.12731g^3 + 0.6993g^4 - 4.689g^5 + 38.44g^6 + \mathcal{O}(g^7)$
4	$0.16667g^2 - 0.16667g^3 + 0.9028g^4 - 6.563g^5 + 55.93g^6 + \mathcal{O}(g^7)$

grouped into two equal pairs—according to the interaction term $(\phi^2)^2$. Hence,

$$\mathcal{C}_G = \sum_{i_1,\ldots,i_{E(G)}=1}^{n} \prod_{v\in V(G)} \lambda(i_{v^{[1]}}, \ldots i_{v^{[4]}}) \tag{13}$$

gives the group factor for vacuum (i.e. 4-regular) graphs, with

$$\lambda(a,b,c,d) \coloneqq \frac{\delta_{a,b}\delta_{c,d} + \delta_{a,c}\delta_{b,d} + \delta_{a,d}\delta_{b,c}}{3}. \tag{14}$$

For a propagator (two-point) graph G, let $\hat{G}$ denote the vacuum graph obtained by gluing the external legs together, and for a vertex (four-point) graph G, let $\hat{G}$ denote the graph obtained by attaching all external legs to an additional vertex (this is known as the *completed* graph [47]). Then it is easy to check that

$$\mathcal{C}_G = \mathcal{C}_{\hat{G}} \cdot \begin{cases} \frac{1}{n} & \text{if } G \text{ is a propagator graph, and} \\ \frac{3}{n(n+2)} & \text{if } G \text{ is a vertex graph.} \end{cases} \tag{15}$$

IV. RESULTS FOR THE RG FUNCTIONS

We now present our results for the six-loop renormalization group functions, computed in the MS scheme in $D = 4 - 2\varepsilon$ dimensions. Among those, the anomalous dimension of the field takes the simplest form, because it only involves Riemann zeta values $\zeta_k = \sum_{n=1}^{\infty} 1/n^k$:

$$\begin{aligned}\gamma_\phi^{\mathrm{MS}}(g) = {} & \frac{n+2}{36}g^2 - \frac{(n+8)(n+2)}{432}g^3 - \frac{5(n^2-18n-100)(n+2)}{5184}g^4 \\ & - [1152(5n+22)\zeta_4 - 48(n^3-6n^2+64n+184)\zeta_3 + (39n^3+296n^2+22752n+77056)]\frac{(n+2)g^5}{186624} \\ & - [512(2n^2+55n+186)\zeta_3^2 - 6400(2n^2+55n+186)\zeta_6 + 4736(n+8)(5n+22)\zeta_5 \\ & - 48(n^4+2n^3+328n^2+4496n+12912)\zeta_4 + 16(n^4-936n^2-4368n-18592)\zeta_3 \\ & + (29n^4+794n^3-30184n^2-549104n-1410544)]\frac{(n+2)g^6}{746496} + \mathcal{O}(g^7).\end{aligned} \tag{16}$$

Note that this result was already obtained in [21] with different methods; so our computation provides a nontrivial check. Numeric values for $n \in \{0,1,2,3,4\}$ are given in Table II. The following results contain also the double zeta value

$$\zeta_{3,5} \coloneqq \sum_{1\le n<m} \frac{1}{n^3 m^5} \approx 0.037707673, \tag{17}$$

which (conjecturally) cannot be written as a polynomial in Riemann zeta values with rational coefficients [42,51]. Our new results are the coefficient of g^6 in the anomalous dimension of the mass (see Table III for numeric expansions):

TABLE III. Numerical values for the six-loop mass anomalous dimension.

n	$\gamma_{m^2}^{\mathrm{MS}}(g)$
0	$-0.6667g + 0.5556g^2 - 2.056g^3 + 10.76g^4 - 75.70g^5 + 636.7g^6 + \mathcal{O}(g^7)$
1	$-1.0000g + 0.8333g^2 - 3.500g^3 + 19.96g^4 - 150.8g^5 + 1355g^6 + \mathcal{O}(g^7)$
2	$-1.3333g + 1.1111g^2 - 5.222g^3 + 31.87g^4 - 255.8g^5 + 2434g^6 + \mathcal{O}(g^7)$
3	$-1.6667g + 1.3889g^2 - 7.222g^3 + 46.64g^4 - 394.9g^5 + 3950g^6 + \mathcal{O}(g^7)$
4	$-2.0000g + 1.6667g^2 - 9.500g^3 + 64.39g^4 - 571.9g^5 + 5983g^6 + \mathcal{O}(g^7)$

$$\gamma_{m^2}^{\overline{\rm MS}}(g) = -\frac{(n+2)g}{3} + \frac{5(n+2)g^2}{18} - \frac{(5n+37)(n+2)g^3}{36}$$
$$+ [288(5n+22)\zeta_4 + 48(3n^2+10n+68)\zeta_3 - (n^2-7578n-31060)]\frac{(n+2)g^4}{7776}$$
$$- [9600(2n^2+55n+186)\zeta_6 - 768(2n^2+145n+582)\zeta_3^2 - 768(5n^2-14n-72)\zeta_5$$
$$- 288(3n^3-29n^2-816n-2668)\zeta_4 + 48(17n^3+940n^2+8208n+31848)\zeta_3$$
$$+ (21n^3+45254n^2+1077120n+3166528)]\frac{(n+2)g^5}{186624} + [1152(14n^2+189n+526)(2063\zeta_8 - 144\zeta_{3,5})$$
$$- 921600(15n^2+239n+718)\zeta_3\zeta_5 - 640(1080n^3+25180n^2+284525n+814062)\zeta_7$$
$$- 15360(2n^3-157n^2-2512n-8268)\zeta_3\zeta_4 + 5120(27n^3+1082n^2+13072n+40008)\zeta_3^2$$
$$+ 3200(285n^3+7178n^2+73768n+196032)\zeta_6 + 320(45n^4+3622n^3+12202n^2+207708n+753040)\zeta_5$$
$$- 240(47n^4+2606n^3-5480n^2-194320n-489328)\zeta_4$$
$$- 80(51n^4-9208n^3-419076n^2-3342688n-8997136)\zeta_3$$
$$- 5(43n^4+48234n^3-5154216n^2-63140784n-145482928)]\frac{(n+2)g^6}{9331200} + \mathcal{O}(g^7) \quad (18)$$

and the coefficient of g^7 in the beta function

$$\beta^{\overline{\rm MS}}(g) = -2\varepsilon g + \frac{n+8}{3}g^2 - \frac{3n+14}{3}g^3 + \frac{96(5n+22)\zeta_3 + 33n^2 + 922n + 2960}{216}g^4$$
$$- [1920(2n^2+55n+186)\zeta_5 - 288(n+8)(5n+22)\zeta_4$$
$$+ 96(63n^2+764n+2332)\zeta_3 - (5n^3-6320n^2-80456n-196648)]\frac{g^5}{3888}$$
$$+ [112896(14n^2+189n+526)\zeta_7 - 768(6n^3+59n^2-446n-3264)\zeta_3^2$$
$$- 9600(n+8)(2n^2+55n+186)\zeta_6 + 256(305n^3+7466n^2+66986n+165084)\zeta_5$$
$$- 288(63n^3+1388n^2+9532n+21120)\zeta_4$$
$$- 16(9n^4-1248n^3-67640n^2-552280n-1314336)\zeta_3$$
$$+ (13n^4+12578n^3+808496n^2+6646336n+13177344)]\frac{g^6}{62208}$$
$$- [204800(1819n^3+97823n^2+901051n+2150774)\zeta_9$$
$$+ 14745600(n^3+65n^2+619n+1502)\zeta_3^3$$
$$+ 995328(42n^3+2623n^2+25074n+59984)\zeta_{3,5}$$
$$- 20736(28882n^3+820483n^2+6403754n+14174864)\zeta_8$$
$$- 5529600(8n^3-635n^2-9150n-25944)\zeta_3\zeta_5$$
$$+ 11520(440n^4+126695n^3+2181660n^2+14313152n+29762136)\zeta_7$$
$$+ 207360(n+8)(6n^3+59n^2-446n-3264)\zeta_3\zeta_4$$
$$- 23040(188n^4+132n^3-93363n^2-862604n-2207484)\zeta_3^2$$
$$- 28800(595n^4+20286n^3+277914n^2+1580792n+2998152)\zeta_6$$
$$+ 5760(4698n^4+131827n^3+2250906n^2+14657556n+29409080)\zeta_5$$
$$+ 2160(9n^5-1176n^4-88964n^3-1283840n^2-6794096n-12473568)\zeta_4$$
$$- 720(33n^5+2970n^4-477740n^3-10084168n^2-61017200n-117867424)\zeta_3$$
$$- 45(29n^5+22644n^4-3225892n^3-88418816n^2-536820560n-897712992)]\frac{g^7}{41990400} + \mathcal{O}(g^8) \quad (19)$$

TABLE IV. Numerical values for the six-loop beta function.

n	$\beta^{\mathrm{MS}}(g)$
0	$-2\varepsilon g + 2.667g^2 - 4.667g^3 + 25.46g^4 - 200.9g^5 + 2004g^6 - 23315g^7 + \mathcal{O}(g^8)$
1	$-2\varepsilon g + 3.000g^2 - 5.667g^3 + 32.55g^4 - 271.6g^5 + 2849g^6 - 34776g^7 + \mathcal{O}(g^8)$
2	$-2\varepsilon g + 3.333g^2 - 6.667g^3 + 39.95g^4 - 350.5g^5 + 3845g^6 - 48999g^7 + \mathcal{O}(g^8)$
3	$-2\varepsilon g + 3.667g^2 - 7.667g^3 + 47.65g^4 - 437.6g^5 + 4999g^6 - 66243g^7 + \mathcal{O}(g^8)$
4	$-2\varepsilon g + 4.000g^2 - 8.667g^3 + 55.66g^4 - 533.0g^5 + 6318g^6 - 86768g^7 + \mathcal{O}(g^8)$

with numeric values given in Table IV. The expansions (16), (18) and (19) are available in computer-readable form in the attached files (see Appendix A).

A. Checks

Our computation exactly reproduced the full five-loop results [10–12,14] and the six-loop field anomalous dimension [21], which in turn is consistent with the first three terms in the large n expansion of the critical exponent η from [52–54]. The leading and subleading terms in the large n expansion of the six-loop beta function, computed almost 20 years ago in [55,56], provided a further successful check.

In addition, we confirmed Broadhurst's results for the MS-renormalized five-loop propagator, obtained in 1993. In fact, in [57] he obtained the ε expansions of all five-loop propagator integrals with ≤ 5 loops, including the finite parts.[6] These results agree perfectly with our ε expansions for those graphs.

A particularly strong check of our results is due to Schnetz [26], who computed β and γ_ϕ to six loops for the case $n = 1$, using completely different techniques including single-valued integration and graphical functions [46].

Also, we initially computed all necessary integrals with a combination of

(i) integration by parts (IBP) [58],
(ii) ε expansions of four-loop massless propagators [59–61],
(iii) IRR extended by the $\mathcal{R}^*$ operation [62–66] and
(iv) parametric integration, using hyperlogarithms, of primitive (free of subdivergences) linear combinations of graphs; examples of this technique are given in graphs M, $M_{3,5}$ and $M_{5,1}$ in [44] and Sec. 5.3.2 in [67].

Together with our more recent strategy [22] of parametric integration with the one-scale scheme, we have in fact computed all diagrams with at least two different exact methods ourselves. In addition, the most complicated diagrams were also checked numerically using sector decomposition [68] to at least three significant digits, using a computer program by the first author. We furthermore cross-checked our generation of the Feynman graphs and their symmetry factors with GraphState by comparison with the output of the program FEYNGEN from [69]. Our numbers of two- and four-point graphs in Table I agree with the lists in [40] (after discarding the tadpole contributions). The $O(n)$ group factors were confirmed independently by evaluating (13) with a simple Form [70] program.

Also, we verified that, after explicitly expanding $\beta(g,\varepsilon) = -2\varepsilon/[\partial_g \log(gZ_g)]$ from (4) and $\gamma_i(g) = \beta(g)\partial_g \log Z_i(g)$ from (5) as series in g, all poles in ε cancel and the results indeed coincide with the final expressions in (4) and (5) in terms of the residues $Z_{i,1}$. This shows that all higher-order poles of the Z factors are consistent with the first-order poles as dictated by the renormalization group.

Finally, we find our results for the six-loop coefficients of the RG functions to be in good agreement with various past predictions based on the ≤ 5-loop coefficients. For example, $\beta_7^{\mathrm{MS}} \approx 34400$ [10] and $\beta_7^{\mathrm{MS}} \approx 34393$ [71] for the case $n = 1$ are very close to our value 34776, where $\beta^{\mathrm{MS}} = \sum_k (-g)^k \beta_k^{\mathrm{MS}}$. Even more interestingly, *asymptotic Padé-approximant predictions* (APAPs) were provided for various values of n in [72,73], as summarized in Table V. In the case of the beta function, we see indeed only very small deviations ($\lesssim 2\%$) from our exact results. It seems plausible to expect that the APAP method might provide potentially even more accurate predictions for the seven-loop coefficient.

For the anomalous dimensions, the APAP forecasts are still reasonable though significantly less precise, as was already noted and discussed in [73] at the five-loop level.[7] In this context let us point out that a qualitatively similar situation occurs for predictions based on the conformal Borel technique: the five- and six-loop predictions [71] (at $n = 1$) for the beta function are good within 1%, whereas the error of the predictions [21] for η increases from 0.5% for six loops to 2.5% for seven loops (according to the seven-loop result for η given in [26]).

[6] We are very thankful to David Broadhurst for making his notes available to us.

[7] The outlyingly large deviations in γ_{m^2} for $n = 4$ and $n = 5$ at six loops are caused by a pole of the Padé approximant at $n \approx 4.7$; the agreement becomes much better again for $n = 6$ and $n = 7$. We are grateful to the authors of [73] for their correspondence and investigation of this matter. In conclusion, the discrepancy at $n = 5$ is very likely an artifact of the Padé method than an indicator of an error in our result for γ_m^2.

TABLE V. Our six-loop coefficients of the RG functions, compared to asymptotic Padé-approximant predictions from [72,73]. The errors are given as (APAP − exact)/exact.

n	0	1	2	3	4	5
β_7^{MS}	23315	34776	48999	66243	86768	110840
APAP [72]	23656	35374	49916	67604	88660	
Error	1.46%	1.72%	1.87%	2.06%	2.18%	
APAP [73]		35233	49381	66426	86636	110292
Error		1.31%	0.78%	0.28%	−0.15%	−0.50%
$\gamma_{m^2}^{\mathrm{MS}}$		1355	2434	3950	5983	8618
APAP [73]		1478	2740	4803	9476	−3374
Error		9%	13%	22%	58%	−139%
$\gamma_{\phi}^{\mathrm{MS}}$		14.4	24.7	38.4	55.9	77.5
APAP [73]		11.2	20.7	35.0	56.2	87.3
Error		−22.0%	−16.3%	−8.9%	0.5%	12.6%

In the following, we discuss the dependence of the RG function coefficients on the perturbative order and on the internal degrees of freedom. We will see that our results are consistent with the expected behavior.

B. Asymptotics

It has long been known that the renormalization group functions are asymptotic series in the coupling g, with factorially growing coefficients [74,75]. For the minimal subtraction scheme, the precise leading asymptotic behavior was first computed in [76] using $4-2\varepsilon$ dimensional instantons [77]. Namely, if we denote the coefficients of the beta function by $\beta^{\mathrm{MS}}(g)=\sum_k \beta_k^{\mathrm{MS}}(-g)^k$, then

$$\beta_k^{\mathrm{MS}} \sim \bar{\beta}_k := k!\cdot k^{3+n/2}\cdot C_\beta \quad \text{as} \quad k\to\infty \tag{20}$$

where C_β is a constant that only depends on the number n of field components:

$$C_\beta = \frac{36\cdot 3^{(n+1)/2}}{\pi\Gamma(2+n/2)A^{2n+4}}\exp\left[-\frac{3}{2}-\frac{n+8}{3}\left(\gamma_{\mathrm{E}}+\frac{3}{4}\right)\right]. \tag{21}$$

In this expression, $\gamma_{\mathrm{E}}=-\Gamma'(1)\approx 0.577$ denotes the Euler-Mascheroni constant and $A\approx 1.282$ is the Glaisher-Kinkelin constant defined by

$$\ln A = \frac{1}{12}-\zeta'(-1)=\frac{1}{12}\left(\gamma_{\mathrm{E}}+\ln(2\pi)-\frac{\zeta'(2)}{\zeta(2)}\right). \tag{22}$$

It is well known that the perturbative coefficients reach their asymptotics rather slowly in the ϕ^4 model [78,79], which is illustrated in Fig. 1 and Table VI. We see that, even at six loops, the ratio $\beta_7^{\mathrm{MS}}/\bar{\beta}_7\approx 0.31$ is still far from one. One also should bear in mind that, at such low perturbative orders, this kind of ratio depends significantly on the function used to model the asymptotic behavior (Fig. 4 in [79]). For illustration, we include in Fig. 1 a comparison of β_k^{MS} to

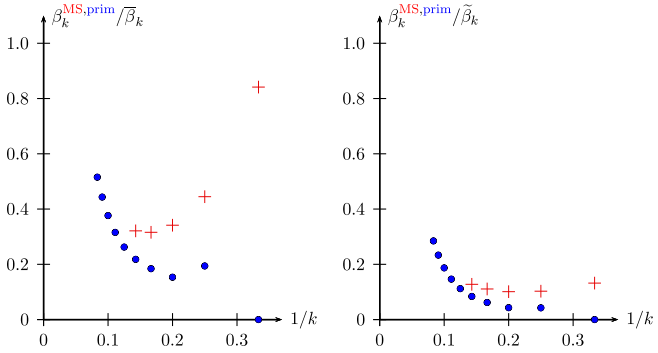

FIG. 1. These plots demonstrate that the perturbative coefficients of the β function ($n=1$) are rather far from their asymptotic values: crosses show the known coefficients β_k^{MS} ($k\le 7$) and circles indicate the estimates for the primitive contributions β_k^{prim} up to loop order 11 (see Table XIII). They are normalized by the predictions from the asymptotic formulas (20) (left plot) and (23) (right plot). The abscissa is $1/k$, such that in the limit $k\to\infty$ the points should approach 1.0 on the vertical axis. Note that there are no primitives with two loops, resulting in the point $(1/3,0)$.

$$\tilde{\beta}_k := \Gamma(k+4+n/2)\cdot C_\beta, \tag{23}$$

which is another reasonable function with the same asymptotics as (20).

In order to probe the asymptotic regime further, we studied the *primitive* contributions β_k^{prim} to β_k^{MS}, that is, the sum of the contributions of all four-point ϕ^4 graphs that are free of subdivergences. These dominate the leading asymptotics of β_k^{MS} as $k\to\infty$, according to page 1865 in [76][8]:

> *In the context of high-order estimates in the perturbative series, we interpret the extra pole in ε as the one produced by the totally irreducible diagrams at high orders. These diagrams are known to be the dominant ones at Kth order for K large for $d<4$ and moreover diverge only like $1/\varepsilon$.*

Indeed, the last row of Table VI shows how the primitive graphs become more and more relevant as the loop number increases.[9] At six loops, the primitive graphs β_7^{prim} already constitute 69% of the coefficient β_7^{MS}. The primitive contributions at seven loops are known exactly [48] and included in Fig. 1.

[8] See also page 15 in [74]: "Finally, the leading diagrams at order K give a single power of $\ln\Lambda$, they are those which do not involve any divergent subgraph; i.e., they are the completely irreducible diagrams."

[9] Such a comparison was already made in evaluation of the four-loop calculation; see [79].

TABLE VI. The upper part of the table shows the ℓ-loop coefficients $\beta^{\rm MS}_{\ell+1}$ of the ϕ^4 beta function $\beta^{\rm MS} = \sum_k \beta^{\rm MS}_k (-g)^k$ (with $n = 1$) and their ratios to the asymptotic formulas (20) and (23). In the lower two rows we show the contribution $\beta^{\rm prim}_{\ell+1}$ containing only the primitive graphs and their proportion of the full ℓ-loop coefficient.

Loop order ℓ	1	2	3	4	5	6
$\beta^{\rm MS}_{\ell+1}/\bar{\beta}_{\ell+1}$ in %	548	83.5	43.8	33.5	30.9	31.4
$\beta^{\rm MS}_{\ell+1}/\tilde{\beta}_{\ell+1}$ in %	43.1	12.5	9.58	9.41	10.4	12.1
$\beta^{\rm MS}_{\ell+1}$	3	5.67	32.5	272	2849	34776
$\beta^{\rm prim}_{\ell+1}$	3	0	14.4	124	1698	24130
$\beta^{\rm prim}_{\ell+1}/\beta^{\rm MS}_{\ell+1}$ in %	100	0	44.3	45.8	59.6	69.4

Furthermore, we were able to obtain accurate numeric estimates for all primitive graphs with up to 11 loops, using a new method (based on the so-called *Hepp bound*) recently introduced by the second author. A brief sketch of this technique is provided in Appendix B. We see in Fig. 1 that, even at 11 loops, the primitive contributions (which are expected to be close to the full $\beta^{\rm MS}_{12}$) reach merely about half of the value predicted by the asymptotic formula (20). Details are given in Table XIII.

We conclude that it is not clear how the knowledge of the leading asymptotic behavior of the perturbative coefficients might be used to accurately predict perturbative coefficients at higher orders. It is thus interesting to note that, in principle, corrections to the leading asymptotic behavior of the form

$$\beta^{\rm MS}_k \sim k! \cdot k^{3+n/2} \cdot C_\beta \left(1 + \sum_{j=1}^{\infty} \frac{a_j}{k^j}\right) \quad \text{as} \quad k \to \infty \qquad (24)$$

can indeed be calculated. In fact, the first correction a_1 was computed long ago in [80] for the momentum subtraction scheme and much more recently in [81] for the MS scheme, using a method developed in [82]. Unfortunately, these results need to be adjusted[10] and we therefore cannot presently discuss if the term a_1/k narrows the gap between the exactly known low-order coefficients $\beta^{\rm MS}_k$ and the asymptotic predictions. This correction could also inflate the gap, because the expansion (24) is itself only asymptotic [83,84] and as such only guarantees an improved fit for very large perturbative orders k.

In particular, we like to stress that the idea to truncate (24), fit the coefficients a_j to make this polynomial in $1/k$ match the known low-order perturbative terms and then use this polynomial to predict (extrapolate) higher-order perturbative coefficients is not justified.[11] For a detailed discussion and criticism of such a procedure, see [85,86].

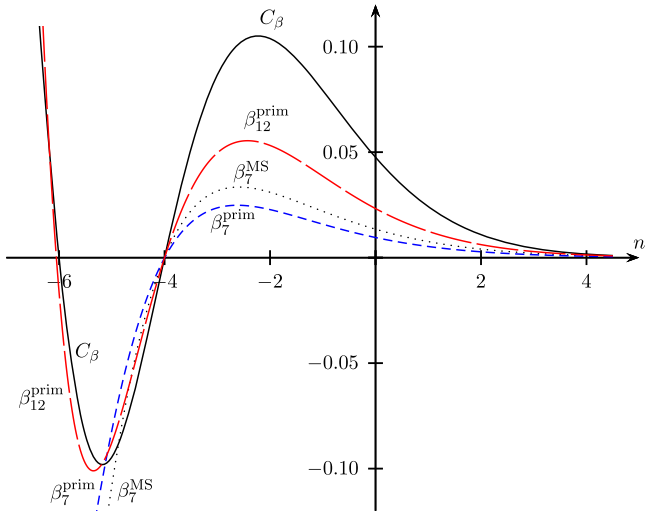

FIG. 2. Dependence of the coefficients of the beta function on n: The dashed curves show the primitive contributions $\beta^{\rm prim}_k/(k! \cdot k^{3+n/2})$ at six and 11 loops. For comparison with the full beta function, our result for $\beta^{\rm MS}_k/(k! \cdot k^{3+n/2})$ at six loops is included as the dotted line. The solid line shows the limiting curve for $k \to \infty$, namely C_β from (21).

C. Dependence on n

The coefficients $\beta^{\rm MS}_k = \beta^{\rm MS}_k(n)$ are functions of the number n of fields, because the contribution of each Feynman graph is multiplied with a corresponding group factor (15). More precisely, $\beta^{\rm MS}_k(n)$ is a polynomial in n for each order k, as seen in (19). Once normalized by the asymptotic growth $k! \cdot k^{3+n/2}$ from (20), these coefficients approach C_β in the limit $k \to \infty$. Since this limit is dominated by the primitive graphs, our estimates for $\beta^{\rm prim}_k$ should exhibit the same behavior.

Figure 2 shows that these expectations are indeed fulfilled. First, we note that the observation (from Fig. 1 at $n = 1$) that even the 11th perturbative order is far from the asymptotic regime extends to all $n \gtrsim -3$. However, all curves share a zero at $n \approx -4$, and the primitive contributions with 11 loops vanish also near to the next zero of C_β at $n = -6$. We note that the asymptotic coefficient C_β is approximated rather well by the primitive contributions $\beta^{\rm prim}_{12}$ in the intermediate region where $-6 < n < -4$.

[10] In particular, in both of these papers, the value of $U_{\rm reg}$ needs to be corrected to $\frac{n+8}{6}(\gamma_{\rm E} + 5/3 + \ln\pi)$, as was kindly pointed out to us by Nalimov. Note that, with this correction, the result for the leading asymptotics computed in [81] coincides with (20) and (21) from [76].

[11] Because (24) is asymptotic, it should be expected that longer truncations with the correct values of a_j yield increasingly worse predictions for the low-order perturbative coefficients. Hence, forcing these to be matched requires the fitted a_j to deviate from their exact values, so there is no reason why those should result in good predictions for higher-order k.

TABLE VII. The first zeros of the exactly known perturbative coefficients $\beta^{\mathrm{MS}}_{\ell+1}$ from (19) as functions of n, for $\ell \le 6$ loops, and similarly for our estimates $\beta^{\mathrm{prim}}_{\ell+1}$ for the primitive contributions from Appendix B (up to 11 loops).

	Loop order ℓ	First zero	Second zero	Third zero
$\beta^{\mathrm{MS}}_{\ell+1}(n)$	1	−8		
	2	−4.67		
	3	−4.025	−41.4	
	4	−4.020	−12.1	3219
	5	−4.0017	−8.76	−44.0
	6	−4.00044	−7.52	−20.0
$\beta^{\mathrm{prim}}_{\ell+1}(n)$	6	−3.99754	−7.22	−35.6
	7	−3.99982	−6.58	−15.1
	8	−3.99994	−6.31	−10.8
	9	−3.999997	−6.18	−9.24
	10	−3.99999991	−6.10	−8.55
	11	−4.000000095	−6.05	−8.21

This phenomenon of zeros at certain values of n was observed in [87] and follows simply from the factor $\Gamma(2+n/2)$ in the denominator of (21), since it implies that C_β, which governs the asymptotic behavior of β^{MS}_k according to (20), vanishes at even values of $n \le -4$. Indeed, the zero of $\beta^{\mathrm{MS}}_{\ell+1}(n)$ that is closest to the origin converges rapidly towards -4 as ℓ increases, which was checked for $\ell \le 5$ loops in [87]. In Table VII, we see that this trend continues at $\ell = 6$ loops and, with an impressive rate of convergence, the same phenomenon continues in our estimates of the primitive contributions $\beta^{\mathrm{prim}}_{\ell+1}$ up to $\ell = 11$ loops. Furthermore, at these higher loop orders, we can see the convergence of the next zeros to the expected values $n = -6$ and $n = -8$.

Note that the group factors $\mathcal{C}_G$ can be negative for such values of n, and in fact only because of these opposite signs is the cancellation of $\beta^{\mathrm{prim}}_{\ell+1}(n)$ possible at all. As a collective phenomenon, sensitive to all Feynman periods at loop order ℓ, we thus interpret the convergence of zeros in Table VII towards even values of $n \le -4$ as a strong consistency check of our exact six-loop results and also of our estimates for the primitive contributions up to 11 loops.

V. RESUMMATION OF CRITICAL EXPONENTS

From the renormalization group functions γ_ϕ, γ_{m^2} and β in Sec. IV, it is straightforward to work out the ε expansions of critical exponents. We focus on η, ν^{-1} and ω, for which (8) and (7) yield the results shown in Tables VIII–X.

The ε expansion $f(\varepsilon) = \sum_{k=0}^{\infty} f_k(-2\varepsilon)^k$ of a critical exponent f around $D = 4 - 2\varepsilon$ dimensions is a formal power series with factorially growing coefficients

$$f_k \sim C_f \cdot k! \cdot a^k \cdot k^{b_f} \quad \text{as} \quad k \to \infty. \tag{25}$$

In fact, this leading asymptotic behavior is completely determined by the asymptotics (20) of the beta function, the leading terms (9) of the perturbation series and the defining equations (6)–(8).[12] In particular, all the coefficients C_f can be expressed as multiples of C_β from (21) and were all computed in [76]. The values of a and the exponents b_f were already obtained in [74]:

$$a = \frac{3}{n+8} \quad \text{and} \quad b_f = \begin{cases} 3 + n/2 & \text{for } f = \eta, \\ 4 + n/2 & \text{for } f = \nu^{-1}, \\ 5 + n/2 & \text{for } f = \omega. \end{cases} \tag{26}$$

In order to obtain estimates for the critical exponents in $D = 3$ dimensions, we must resum the divergent series $f(\varepsilon)$ at $\varepsilon = 1/2$.

This problem of resummation is a huge subject (see for example the review [89]), and many different approaches have been put forward. Unfortunately, no consensus has so far been reached on the optimal method to resum ε expansions. We therefore think that a careful comparison of the various methods, based on the six-loop perturbation series presented here, would be very valuable. In particular in view of the potential for further higher-order perturbative computations in the near future, like the seven-loop ε expansions in the ϕ^4 model [26], such further insight into the resummation problem is very desirable.

However, such an extensive analysis would exceed the scope of this article and we decided to discuss only the method of Borel resummation with conformal mapping. It would be very interesting to see how other approaches, including order-dependent mapping [90,91], large-coupling expansions [92–94] and self-similar factor approximants [95], fare with the six-loop perturbative input.

A. Borel resummation with conformal mapping

We will describe the method introduced first in [79] for the resummation of series in the coupling g and then also applied to ε expansions [9]. This technique has a successful history in the resummation of critical exponents [6,13,16,96] and is explained in detail for example in Chap. 16 in [1].

To begin with, we denote the *Borel transform* of $f = \sum_{k=0}^{\infty} f_k(-2\varepsilon)^k$ as

$$\mathfrak{B}^b_f(x) := \sum_{k=0}^{\infty} \frac{f_k}{\Gamma(k+b+1)}(-x)^k. \tag{27}$$

According to (25), it defines an analytic function in the domain $|x| < 1/a$ with a singularity at $x = -1/a$ of the

[12] Equations (6)–(8) furthermore relate corrections to the leading asymptotics, as for example computed in [81]. If one encodes the full asymptotic expansions as generating functions, these relations can be computed elegantly in an algebraic way [88].

TABLE VIII. Numerical six-loop ε expansion of the critical exponent η in $D = 4 - 2\varepsilon$ dimensions.

n	$\eta(\varepsilon)$
0	$0.062500\varepsilon^2 + 0.13281\varepsilon^3 - 0.13388\varepsilon^4 + 0.84815\varepsilon^5 - 5.8067\varepsilon^6 + \mathcal{O}(\varepsilon^7)$
1	$0.074074\varepsilon^2 + 0.14952\varepsilon^3 - 0.13326\varepsilon^4 + 0.82101\varepsilon^5 - 5.2014\varepsilon^6 + \mathcal{O}(\varepsilon^7)$
2	$0.080000\varepsilon^2 + 0.15200\varepsilon^3 - 0.12630\varepsilon^4 + 0.74269\varepsilon^5 - 4.3921\varepsilon^6 + \mathcal{O}(\varepsilon^7)$
3	$0.082645\varepsilon^2 + 0.14719\varepsilon^3 - 0.11919\varepsilon^4 + 0.65225\varepsilon^5 - 3.6495\varepsilon^6 + \mathcal{O}(\varepsilon^7)$
4	$0.083333\varepsilon^2 + 0.13889\varepsilon^3 - 0.11336\varepsilon^4 + 0.56421\varepsilon^5 - 3.0312\varepsilon^6 + \mathcal{O}(\varepsilon^7)$

TABLE IX. Numerical six-loop ε expansion of the critical exponent $1/\nu$ in $D = 4 - 2\varepsilon$ dimensions.

n	$\nu^{-1}(\varepsilon)$
0	$2.0000 - 0.50000\varepsilon - 0.34375\varepsilon^2 + 0.91540\varepsilon^3 - 4.6002\varepsilon^4 + 30.596\varepsilon^5 - 246.77\varepsilon^6 + \mathcal{O}(\varepsilon^7)$
1	$2.0000 - 0.66667\varepsilon - 0.46914\varepsilon^2 + 0.99622\varepsilon^3 - 4.9096\varepsilon^4 + 30.440\varepsilon^5 - 228.65\varepsilon^6 + \mathcal{O}(\varepsilon^7)$
2	$2.0000 - 0.80000\varepsilon - 0.56000\varepsilon^2 + 0.97949\varepsilon^3 - 4.8756\varepsilon^4 + 28.136\varepsilon^5 - 198.59\varepsilon^6 + \mathcal{O}(\varepsilon^7)$
3	$2.0000 - 0.90909\varepsilon - 0.62359\varepsilon^2 + 0.92057\varepsilon^3 - 4.6976\varepsilon^4 + 25.278\varepsilon^5 - 168.91\varepsilon^6 + \mathcal{O}(\varepsilon^7)$
4	$2.0000 - 1.00000\varepsilon - 0.66667\varepsilon^2 + 0.84684\varepsilon^3 - 4.4586\varepsilon^4 + 22.469\varepsilon^5 - 142.96\varepsilon^6 + \mathcal{O}(\varepsilon^7)$

TABLE X. Numerical six-loop ε expansion of the correction to scaling ω in $D = 4 - 2\varepsilon$ dimensions.

n	$\omega(\varepsilon)$
0	$2.0000\varepsilon - 2.6250\varepsilon^2 + 14.589\varepsilon^3 - 100.57\varepsilon^4 + 859.94\varepsilon^5 - 8320.5\varepsilon^6 + \mathcal{O}(\varepsilon^7)$
1	$2.0000\varepsilon - 2.5185\varepsilon^2 + 12.946\varepsilon^3 - 83.762\varepsilon^4 + 663.99\varepsilon^5 - 5959.1\varepsilon^6 + \mathcal{O}(\varepsilon^7)$
2	$2.0000\varepsilon - 2.4000\varepsilon^2 + 11.497\varepsilon^3 - 70.724\varepsilon^4 + 523.96\varepsilon^5 - 4401.7\varepsilon^6 + \mathcal{O}(\varepsilon^7)$
3	$2.0000\varepsilon - 2.2810\varepsilon^2 + 10.263\varepsilon^3 - 60.498\varepsilon^4 + 421.82\varepsilon^5 - 3341.1\varepsilon^6 + \mathcal{O}(\varepsilon^7)$
4	$2.0000\varepsilon - 2.1667\varepsilon^2 + 9.2207\varepsilon^3 - 52.351\varepsilon^4 + 345.65\varepsilon^5 - 2596.3\varepsilon^6 + \mathcal{O}(\varepsilon^7)$

form $(1+ax)^{b-b_f-1}$. We assume[13] that f is Borel summable, which means that $\mathfrak{B}_f^b(x)$ admits an analytic continuation to the positive real axis $x > 0$ and also includes that the *Borel sum*

$$\tilde{f}(\varepsilon) \coloneqq \int_0^\infty t^b e^{-t} \mathfrak{B}_f^b(2\varepsilon t) \mathrm{d}t \tag{28}$$

converges and gives the correct value of the critical exponent at $\varepsilon = 1/2$, which is our case of interest ($D = 3$). By construction, this Borel sum $\tilde{f}(\varepsilon)$ has the perturbative expansion $f(\varepsilon)$ as required. In order to compute the integral (28), we must analytically continue the Borel transform $\mathfrak{B}_f^b(x)$ from the circle $|x| < 1/a$ of convergence to the positive real line. This is achieved with the conformal transformation

$$w(x) = \frac{\sqrt{1+ax}-1}{\sqrt{1+ax}+1} \quad \text{with inverse } x(w) = \frac{4w}{a(1-w)^2}, \tag{29}$$

as it maps the integration domain $x \in (0, \infty)$ to the interval $w \in (0, 1)$. Assuming that all singularities of $\mathfrak{B}_f^b(x)$ lie on the cut $(-\infty, -1/a]$, which is mapped onto the unit circle $|w| = 1$, the expansion of the Borel transform $\mathfrak{B}_f^b(x(w))$ into a series in w converges in the full integration domain and thus provides the sought-after analytic continuation.

Because we only know the first few expansion coefficients f_k with $k \le 6$, we can only approximate the Borel transform. Following [9,79], we introduce a second parameter λ and the truncation order ℓ to write it as

$$\mathfrak{B}_f^b(x) \approx \mathfrak{B}_f^{b,\lambda,\ell}(x) \coloneqq \left(\frac{ax}{w(x)}\right)^\lambda \sum_{k=0}^{\ell} B_{f,k}^{b,\lambda} [w(x)]^k. \tag{30}$$

The coefficients $B_{f,k}^{b,\lambda}$ are functions of b and λ, determined by matching the coefficients of x^0 through x^ℓ in the expansion of $\mathfrak{B}_f^{b,\lambda,\ell}(x)$ with the perturbative constraints (27). This ensures that $\mathfrak{B}_f^b(x)$ is approximated well for small values of x. Crucially, the parameter λ allows us to also adjust the growth $\mathfrak{B}_f^{b,\lambda,L}(x) \sim x^\lambda$ for large x to better match the behavior of the actual Borel transform. Without this degree of freedom, our approximations $\mathfrak{B}_f^{b,0,\ell}(x) \to \sum_{k=0}^{\ell} B_{f,k}^{b,0}$ would always approach a constant value at

[13]While the Borel summability with respect to the coupling g has been established in the fixed dimensions $D = 2$ [97] and $D = 3$ [98], it remains an open question for the ε expansion.

$x \to \infty$. This appears to model the Borel transform only very poorly, and a careful choice of λ is essential to significantly improve the quality of the resummation [9,71,96].

Our approximate result for the Borel sum (28) is then given by

$$\tilde{f}(\varepsilon) \approx \tilde{f}_\ell^{b,\lambda}(\varepsilon) \coloneqq \int_0^\infty t^b e^{-t} \mathfrak{B}_f^{b,\lambda,\ell}(2\varepsilon t) \mathrm{d}t. \tag{31}$$

Finally, a third parameter was introduced in [13] to improve the results even further. Namely, we consider a *homographic transformation*

$$\varepsilon = h_q(\varepsilon') \coloneqq \frac{\varepsilon'}{1+q\varepsilon'} \quad \text{with inverse } \varepsilon' = h_q^{-1}(\varepsilon) = \frac{\varepsilon}{1-q\varepsilon} \tag{32}$$

to reexpand the original ε expansions as series in ε' (for $q = 0$, nothing changes). We then proceed as above, taking this new series as input:

$$\tilde{f}(\varepsilon) \approx \tilde{f}_\ell^{b,\lambda,q}(\varepsilon) \coloneqq \int_0^\infty t^b e^{-t} \mathfrak{B}_{f\circ h_q}^{b,\lambda,\ell}\left(\frac{2\varepsilon t}{1-q\varepsilon}\right) \mathrm{d}t. \tag{33}$$

The motivation for (32) is that it allows us to map potential singularities of critical exponents as functions of ε further away from the point $\varepsilon = 1/2$, in order to diminish their possibly detrimental influence on the resummation [13].

In closing, let us stress that there are several aspects in which this basic scheme might be adjusted. For example, we could choose other conformal mappings than (29), replace (32) by a different transformation and instead of (30) we could use another class of functions to approximate the Borel transform.[14]

B. Dependence on resummation parameters

Our resummation procedure is formulated in terms of three parameters: b, λ and q. If we knew the full perturbation series of a critical exponent $f(\varepsilon)$, the resummed value $\tilde{f}(\varepsilon) = \lim_{\ell\to\infty} \tilde{f}_\ell^{b,\lambda,q}(\varepsilon)$ would not depend on these choices. But since we only have the first few terms of the ε expansions at hand, we are forced to consider the truncations $\tilde{f}_\ell^{b,\lambda,q}(\varepsilon)$ with $\ell \le 6$. These do depend on the parameters, which therefore have to be chosen carefully.

Let us first comment on b. The asymptotic behavior of the coefficients of our approximations of the Borel transform, $\mathfrak{B}_f^{b,\lambda,\ell}(x)$ from (30), is given by

$$\begin{aligned}\left(\frac{ax}{w(x)}\right)^\lambda [w(x)]^p &= 4^\lambda \left(\frac{ax}{4}\right)^p \sum_{k=0}^\infty \binom{2(k-\lambda+p)}{k} \frac{\lambda-p}{\lambda-p-k} \left(-\frac{ax}{4}\right)^k \\ &= (-1)^p (p-\lambda) \sum_{k=p}^\infty \frac{(-ax)^k}{\sqrt{\pi k^3}} \left(1+\mathcal{O}\left(\frac{1}{k}\right)\right).\end{aligned} \tag{34}$$

It was noted in [79] that we can therefore match the leading asymptotics (25) of the perturbation series and our model for the Borel transform by setting $b = b_f + 3/2$, according to (27) and $\Gamma(k+b+1) \sim k! \cdot k^b$. This fixed value was indeed used in [9,21,71,79,96], with the idea that it incorporates the contributions from very-high-order perturbation theory. We do not follow this strategy, for the following reasons:

(1) For an exact resummation of the high-order contributions, we would actually also have to enforce a precise matching of the constant[15]

$$C_f \overset{!}{=} \frac{1}{\sqrt{\pi}} \sum_{p=0}^L (-1)^p (p-\lambda) B_{f,p}^{b,\lambda}.$$

(2) In Sec. IV B we saw that even six loops remain far away from the asymptotic regime (Fig. 1). The contribution of the resummed asymptotic higher orders is thus likely outweighed by the deviation of the seven-loop contribution from its asymptotic estimate (25).

(3) Variation of the parameter b, as first suggested in [5], can improve the resummation and also provides a hint towards the uncertainty of the result.

Instead, let us investigate how the resummation depends on b. According to (27), the Taylor coefficients of the Borel transform become smaller with increasing b. Since the nontruncated Borel sum does not depend on b, this implies that the dominant contribution to the integral (28) must come from larger values of x. Hence, with increasing b, our model for the large-x behavior of the Borel transform (encoded in the parameter λ) should become more relevant.

Figure 3 demonstrates this behavior, by plotting the resummations $\tilde{\eta}_\ell^{b,\lambda,q}(1/2)$ of the critical exponent η (with various truncation orders ℓ of the ε expansion) as a function of b for several values of λ. First note that, as expected, in each case the dependence on b decreases if we take more terms of the ε expansion into account (it will disappear completely only in the limit $\ell \to \infty$). Furthermore, the choice of λ has a strong influence on the b dependence of the resummation.

[14]For example, hypergeometric functions were proposed in [99] and Chap. 19 in [1]. Furthermore, Padé approximants have been suggested as a replacement for the Taylor series (30); see [100,101].

[15]This was pointed out in [79]. We note that in this reference, the overall sign in Eq. (14) seems wrong, and in Eqs. (13) and (14), a_0 should not appear, according to our (34).

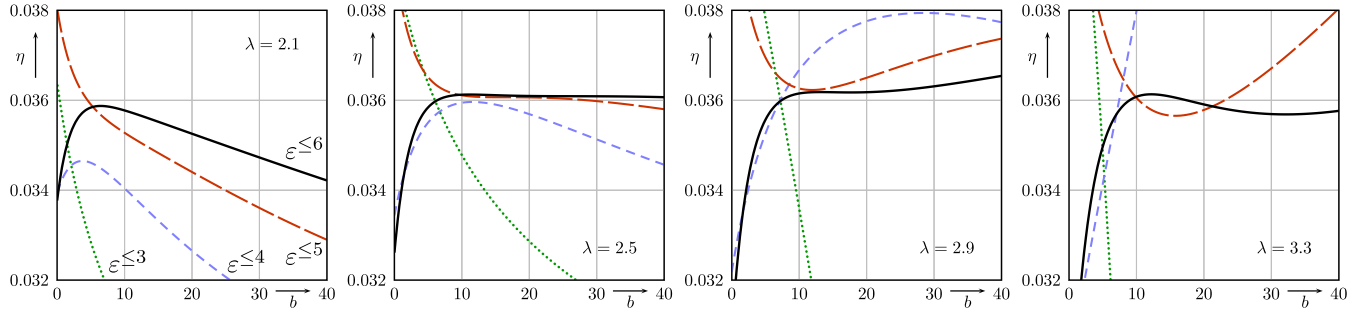

FIG. 3. Dependence of the resummations $\tilde{\eta}_\ell^{b,\lambda,q}$ of η on b for different values of λ, at $n = 1$ in $D = 3$ dimensions ($\varepsilon = 0.5$) with $q = 0.2$. The loop order ℓ is indicated by the label $\varepsilon^{\le\ell}$.

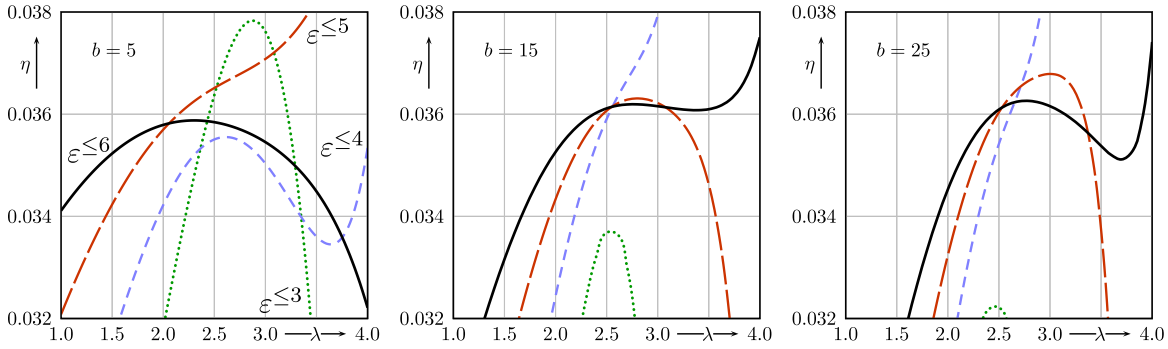

FIG. 4. Dependence of the resummation of η on λ for different values of b, for $n = 1$ in $D = 3$ dimensions with $q = 0.2$. The loop order ℓ is indicated by the label $\varepsilon^{\le\ell}$.

In fact, for most λ's, the dependence on b is very strong. However, we find that for a rather small range of λ, the five- and six-loop resummations become almost insensitive to b as illustrated by the plateau in the second plot of Fig. 3. This stability (with respect to b) deteriorates quickly if we resum fewer terms of the ε expansion. As expected from our discussion earlier, we also see that for larger values of b, the resummation depends more strongly on the tuning of λ. Finally note that with (26), the value $b = b_\eta + 3/2 = 5$ chosen in [9,96] seems too small and misses the plateaus.

In conclusion, we take the sensitivity with respect to b both as an indicator of the uncertainty of the resummation and as a criterion to choose λ and q. This is a common approach in general, and the existence of wide plateaus in this case was for example pointed out in [30].[16] The power of studying the sensitivity with respect to the resummation parameters was also demonstrated in [102], and indeed we will also apply this criterion with respect to variations of λ.

In Fig. 4 we see the dependence of the resummation on λ for various b. As we expect from Fig. 3, very small values like $b = 5$ give a very unstable picture. For suitable larger values like $b = 15$ we find λ intervals where the six-loop resummation $\tilde{\eta}_6$ (and to a lesser degree also the five-loop resummation $\tilde{\eta}_5$) varies only very little. If we further increase b, the curves become more sensitive to λ again. However, even in the plot for $b = 25$, the value at the near-optimal $\lambda = 2.5$ from Fig. 3 remains essentially unchanged.

Finally, it is important to stress the role of the homographic transformation, indexed by q. The reexpansion in ε' after the substitution (32) adjusts the coefficients in a nontrivial way and thereby has a potential to alter the apparent convergence of the resummation procedure. In Fig. 5 we show the dependence on b for various choices of q, where in each case λ was tuned to minimize the sensitivity to b.

The wide plateau existent for $q = 0.2$ (already shown in Fig. 3) gets shorter for larger q and the dependence on b becomes much stronger away from a short range of q near 0.2. Also note that the level of the (shortened) plateaus shifts with q (in Fig. 5, the plateau moves down when q is raised above 0.2). Clearly, such a strong correlation of the resummation result with a free parameter is not desirable. But we see that the stability criterion with respect to b nevertheless clearly singles out a preferred range of q. The same qualitative observation applies to the dependence on λ; that is, for q far from 0.2, the dependence on λ (as in the plots like the ones shown in Fig. 4) becomes stronger.

[16]In [30,102], the same approach was used to optimize the value for a in (29). It was observed that the dependence on a is very weak and that the best choices of a lie very close to the value from (26) in the asymptotic growth (25). We therefore keep a fixed at this value.

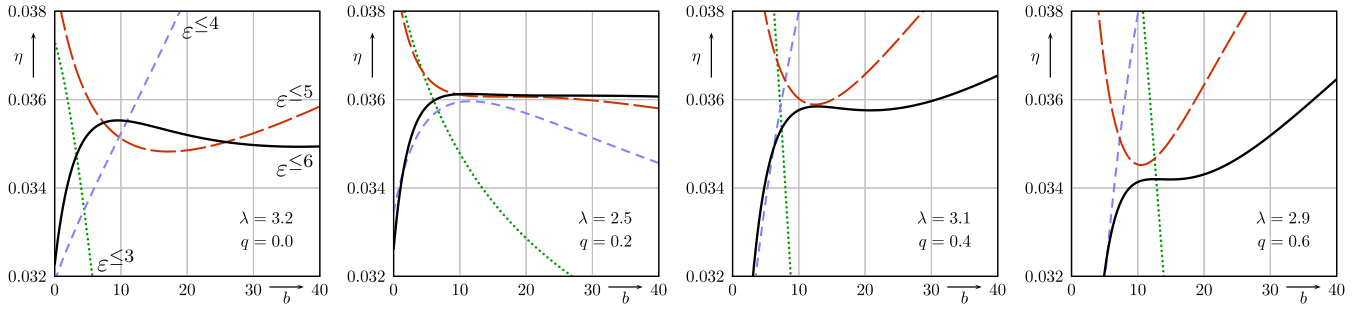

FIG. 5. For different values of $q \in \{0, 0.2, 0.4, 0.6\}$, we plot the dependence of the resummation on b. In each case, we adjusted λ to find the best apparent stability with respect to b. The loop order ℓ is indicated by the label $\varepsilon^{\leq \ell}$.

In summary, we confirm the observation of [13] that the homographic transformation (32), with a suitable choice of q, can significantly improve the apparent stability of the resummation with respect to variations in b and λ. Incidentally, note that the nearly optimal choice (with respect to these stabilities) of setting (b, λ, q) to (15,2.5,0.2) yields a result of $\tilde{\eta}_6^{b,\lambda,q} \approx 0.03611$, which agrees well with earlier resummations and estimates from other methods (see Table XI). Without the homographic transformation, that is $q = 0$, the stability and the agreement with other results would be much worse (see the leftmost plot in Fig. 5).

C. Resummation algorithm

In order to quantify the sensitivity of a function $F(x)$ with respect to a resummation parameter x, we pick a scale Δ_x and define

$$\mathrm{Var}_x(F(x)) \coloneqq \min_{a \leq x \leq a+\Delta_x} \left(\max_{a \leq x' \leq a+\Delta_x} |F(x) - F(x')| \right) \tag{35}$$

as the minimum spread of the values $F(x')$ around $F(x)$ inside an interval $x' \in [a, a + \Delta_x]$ of width Δ_x that contains x (so a runs from $x - \Delta_x$ to x). A smaller value of this quantity corresponds to an increasingly flat plateau (of width Δ_x) in the kind of plots we show above. Following our discussion in Sec. V B, we want to pick the resummation parameters such that these spreads, and in particular $\mathrm{Var}_b(\tilde{f}_\ell^{b,\lambda,q})$, become as small as possible. But this is not the only desirable criterion.

A further indicator for the uncertainty of the resummation is given by the size of the corrections going from one loop order to the next. In fact, in [9,96], λ was determined exclusively by minimizing the relative differences

$$Q_\ell \coloneqq |1 - \tilde{f}_\ell / \tilde{f}_{\ell-1}|$$

of the last few loop orders. Pictorially, this amounts to searching for intersections of the curves labeled $\varepsilon^{\leq 6}$, $\varepsilon^{\leq 5}$ and $\varepsilon^{\leq 4}$ in the plots as shown in Figs. 3 and 4.

These two very general approaches are called *principle of minimum sensitivity* (PMS) [110] and *principle of fastest apparent convergence* (PFAC) [111]. In our context of critical exponents, they are discussed for example in [102], and they can be applied in many different ways. In fact, we found that several works on resummations leave out some of the details of the employed procedure, making it difficult to reproduce the results.[17] Therefore, let us state our method precisely.

We combine both the PMS and the PFAC into the *error estimate*

$$\begin{aligned} E_\ell^f(b, \lambda, q) \coloneqq & \max\{|\tilde{f}_\ell^{b,\lambda,q} - \tilde{f}_{\ell-1}^{b,\lambda,q}|, |\tilde{f}_\ell^{b,\lambda,q} - \tilde{f}_{\ell-2}^{b,\lambda,q}|\} \\ & + \max\{\mathrm{Var}_b(\tilde{f}_\ell^{b,\lambda,q}), \mathrm{Var}_b(\tilde{f}_{\ell-1}^{b,\lambda,q})\} \\ & + \mathrm{Var}_\lambda(\tilde{f}_\ell^{b,\lambda,q}) + \mathrm{Var}_q(\tilde{f}_\ell^{b,\lambda,q}). \end{aligned} \tag{36}$$

The first term accounts for the uncertainty due to the unknown corrections from higher perturbative orders (estimated by the differences of the largest two loop orders), whereas the spreads in the following two lines take care of the arbitrariness in the choice of the parameters b, λ and q. We pick the scales as follows:

(i) $\Delta_b = 20$, because we indeed find such strikingly wide plateaus (with only minute variations of the resummation result), as seen in Fig. 3 and noticed in [30], for all critical exponents and values of n that we considered.

(ii) $\Delta_\lambda = 1$, since the dependence on λ is stronger and even at six loops the plateaus do not grow much longer (see Fig. 4).

(iii) $\Delta_q = 0.02$, as the dependence on q is very strong (for fixed λ); higher values of Δ_q would yield unrealistically high error estimates.

Our resummation of a critical exponent f at order ℓ then proceeds as follows:

(1) Sample $\tilde{f}_\ell^{b,\lambda,q}$ as defined in (33) for parameters in the cube

$$(b, \lambda, q) \in [0, 40] \times [0, 4.5] \times [0, 0.8],$$

where b runs over half-integers and λ and q are probed in steps of 0.02.

[17] Some notable exceptions are [112] and Appendix A in [113], where the scanned parameter ranges are discussed in detail.

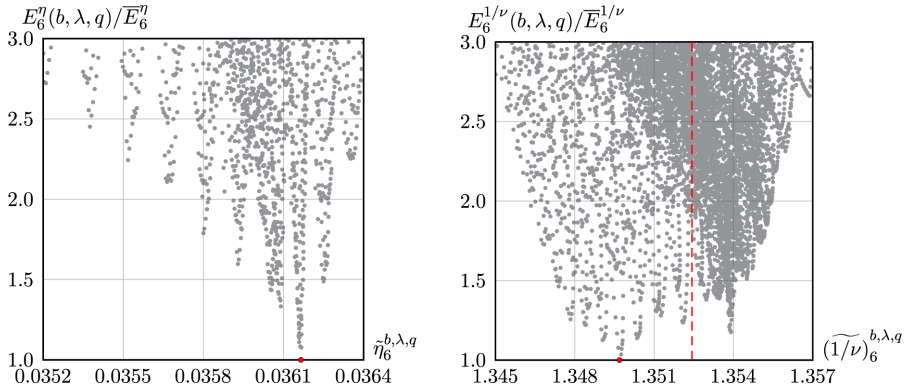

FIG. 6. Six-loop resummation results and their error estimates (36) for the critical exponent η of the Ising model (left plot) and ν^{-1} of the $O(4)$ model (right plot), in three dimensions. In the first case, the "best" resummation is rather sharply localized, whereas the second plot reveals a wide spread among the resummations with small error estimates. The dashed vertical line shows the weighted average.

(2) For each such point (b,λ,q), compute the error estimate (36).
(3) Find the (global) minimum $\bar{E}_\ell^f$ of these values for $E_\ell^f(b,\lambda,q)$.

For the example of η (in the three-dimensional Ising case $n=1$), the "apparently best" resummation, according to our error estimate, occurs at $(b,\lambda,q)=(11,2.56,0.2)$ and yields $\bar{E}_6^{\eta}\approx 0.0002$. These resummation parameters are very close to the second plots in Figs. 3 and 4. The actual value of the resummed critical exponent is $\tilde{\eta}_6^{11,2.56,0.2}\approx 0.03615$ and agrees (within the error estimate $\bar{E}_6^{\eta}$) with results from completely different theoretical approaches (see Table XI).

A comment is due on our choice for the function $E_\ell^f(b,\lambda,q)$, which we use as a quantitative measure for the "quality" of a resummation. Obviously, there are many different reasonable definitions of such a measure.[18] And even if we stay with our definition (36), it still depends on the somewhat arbitrary parameters Δ_b, Δ_λ and Δ_q. However, we tested numerous such variations and found that their effect on the selection of the apparently best resummation parameters (b,λ,q) only results in very small shifts of the critical exponents. Broadhurst attributes a fitting quote to Jean Zinn-Justin (paraphrased):

> *In work on resummation, there is always an undeclared parameter: the number of methods tried and rejected before the paper was written.*

We stopped counting.

D. Error estimates

The estimation of resummation errors is a notoriously difficult undertaking, for mainly two reasons:

(i) We do not know the perturbative coefficients of the next loop order.
(ii) The free parameters (in our case: b, λ and q) can in principle be tuned to reproduce any value for the critical exponents.

Therefore, we can only hope to get a good guess of the error if we assume

(A) the next perturbative correction is not much larger than the last known correction and
(B) the exact critical exponent is close to the resummed critical exponent $\tilde{f}_\ell^{b,\lambda,q}$ when the parameters (b,λ,q) are chosen in order to minimize $E_\ell^f(b,\lambda,q)$.

We chose the widths Δ_b, Δ_λ and Δ_q as given above such that $E_\ell^f(b,\lambda,q)$ from (36) should be considered as a lower bound on the error that is inherent to the resummation $\tilde{f}_\ell^{b,\lambda,q}$. To verify that this guess of the error is self-consistent, we consider plots as shown in Fig. 6, i.e. the critical exponent η of the three-dimensional Ising model ($n=1$). Each point $(\tilde{\eta}_6^{\theta},E_6^{\eta}(\theta))$ represents a set $\theta=(b,\lambda,q)$ of resummation parameters with an error estimate $\leq 0.0006\approx 3\bar{E}_6^{\eta}$. We notice that the optimal resummation ($\tilde{E}_6^{\eta}\approx 0.0002$) is rather sharply localized. The spread of the resummation results around this optimum increases in line with the error estimate—this means that our error estimates are indeed consistent with the actual spread.

But there are also cases, like the critical exponent ν in the $O(4)$ model as illustrated in the right plot of Fig. 6, where there exist many resummation parameters that yield a close to minimal error estimate but which produce results that are spread much more widely than the error estimate suggests. In such a situation, we do not pick the apparently best resummation (like we do for η), but instead we choose a mean value [e.g. 1.352 in the $O(4)$ example] as a more faithful representation of the distribution of resummations. This is how we compiled our resummation data in Table XI in the next section. Similar plots are provided for all exponents in an ancillary file (see Appendix A).

[18]For example, one could incorporate more low-order corrections $|f_\ell - f_{\ell-k}|$ with $k\geq 2$, or disregard the stability $\mathrm{Var}_b(f_{\ell-1})$, or take further stabilities of lower loop orders into account.

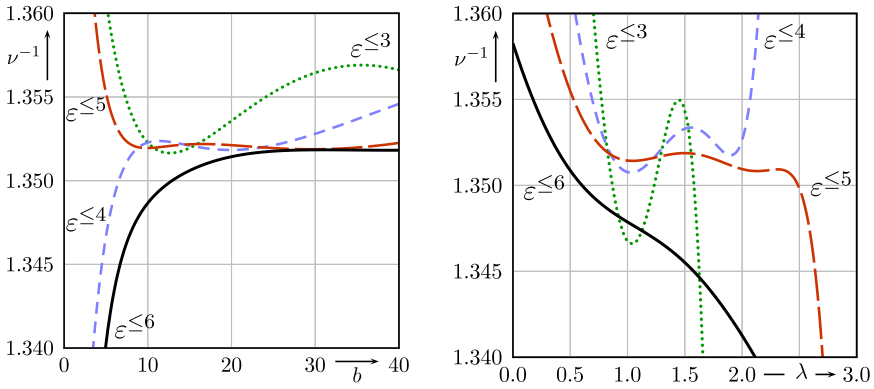

FIG. 7. Dependence of the resummation results for the critical exponent ν^{-1} in the three-dimensional $O(4)$ model on b and λ, around the point $(b, \lambda, q) = (10, 0.82, 0.4)$ of the apparently best five-loop resummation. In this case, the sixth loop order induces a significant correction, which exceeds what one might expect from just considering the variation (as a function of b and λ) intrinsic to the five-loop resummation itself.

In order to take the actual spreads of the best resummations (like shown in Fig. 6) into account, all errors reported in the following section consist of the minimum error estimate $\bar{E}^f_\ell$, plus an additional contribution given by two standard deviations of the set of all resummations with an error $\leq 3\bar{E}^f_\ell$. One might argue that this would overestimate the error, since we aimed to account for the spreads due to variations in the parameters (b, λ, q) already in (36). However, given the arbitrariness in fixing the widths Δ_x and the unknown uncertainties neglected by assuming (A) and (B) above, we are more confident with stating these enlarged errors (in particular since underestimated errors are not uncommon in the literature [114]).

Let us point out in an explicit example how the error predicted by the principles PMS and PFAC, like (36), can underestimate the corrections from higher-order contributions. We consider again the exponent ν in the three-dimensional $O(4)$ model. The apparently best five-loop resummation gives $\nu^{-1} \approx 1.352$ at $\theta = (b, \lambda, q) = (10, 0.82, 0.4)$ with an error estimate of $\bar{E}^{1/\nu}_5 \approx 0.002$. On the scale of Fig. 7, we see indeed only very small fluctuations of the five-loop resummation when b and λ are varied. Furthermore, the three-, four- and five-loop resummations essentially coincide at θ; in other words, the four- and five-loop corrections almost vanish at this point. Nonetheless, we see that the six-loop correction is significant and much larger than the fluctuations of the five-loop result. This kind of behavior appears to be linked with large spreads of the best resummations as shown in the right plot of Fig. 6 and explains why, in some rare cases, our error estimates for the six-loop resummations quoted in Table XI actually exceed the error estimates for the resummations of the five-loop series.

In such a case one could say that the five-loop result *seemed converged*, but towards an erroneous value. This phenomenon is particularly well known to occur in two dimensions, where it was called "anomalous apparent convergence" in [102]. Here we also like to stress that the large-x behavior of the Borel transform $\mathfrak{B}^{b,\lambda,\ell}_f(x)$ of critical exponents f is still unknown. Hence the power law model (30) is only justified because it seems to work very well in practice, but it remains unclear if λ can actually be interpreted as the exponent of a power law asymptotic behavior of $f(\varepsilon)$ for large ε. If the exact large-x behavior is of a different form, then the PMS might miss the correct value (Appendix A in [93]).

VI. ESTIMATES FOR CRITICAL EXPONENTS IN THREE DIMENSIONS

The critical phenomena of many interesting physical systems are described by the $O(n)$ universality classes. We refer to [115] for a comprehensive discussion and only recall some of the most interesting examples:

$n = 0$ *(self-avoiding walks)*.—polymers [116],
$n = 1$ *(Ising universality class)*.—liquid-vapor transitions, uniaxial magnets,
$n = 2$ *(XY universality class)*.—superfluid λ transition of helium [117],
$n = 3$ *(Heisenberg universality class)*.—isotropic ferromagnets,
$n = 4$.—finite temperature QCD with two light flavors [118].

These are the systems that we consider below; larger values of n were discussed for example in [113,119,120].

The critical behavior of each universality class is governed by the critical exponents α, β, γ, δ, η and ν. However, in our field-theoretic approach, only two of them are independent and determine all others through the scaling relations (10). So, while discussing agreement with other theoretical methods, we will only consider the critical exponents η, ν and the correction to scaling exponent ω.

In Table XI, we present the summary of our results for the six-loop resummation of these exponents, in $D = 3$ dimensions for $0 \leq n \leq 4$. For comparison of the

TABLE XI. Estimates for critical exponents in $D = 3$ dimensions of the $O(n)$ vector model. Results from the conformal bootstrap and Monte Carlo techniques are listed first (we tried to collect the most accurate predictions in each case). Our estimates from the five- and six-loop ε expansions are shown next. For comparison of the resummation methods, we display the five-loop results (from ε expansion without $D = 2$ boundary conditions) according to [16].

		$n = 0$	$n = 1$	$n = 2$	$n = 3$	$n = 4$
η		0.031043(3)[a]	0.036298(2)[18]	0.0381(2)[103]	0.0378(3)[104]	0.0360(3)[b]
	ε^6	0.0310(7)	0.0362(6)	0.0380(6)	0.0378(5)	0.0366(4)
	ε^5	0.0314(11)	0.0366(11)	0.0384(10)	0.0382(10)	0.0370(9)
	[16]	0.0300(50)	0.0360(50)	0.0380(50)	0.0375(45)	0.036(4)
ν		0.5875970(4)[20]	0.629971(4)[18]	0.6717(1)[103]	0.7112(5)[105]	0.7477(8)[c]
	ε^6	0.5874(3)	0.6292(5)	0.6690(10)	0.7059(20)	0.7397(35)
	ε^5	0.5873(13)	0.6290(20)	0.6687(13)	0.7056(16)	0.7389(24)
	[16]	0.5875(25)	0.6290(25)	0.6680(35)	0.7045(55)	0.737(8)
ω		0.904(5)[d]	0.830(2)[106]	0.811(10)[e]	0.791(22)[e]	0.817(30)[e]
	ε^6	0.841(13)	0.820(7)	0.804(3)	0.795(7)	0.794(9)
	ε^5	0.835(11)	0.818(8)	0.803(6)	0.797(7)	0.795(6)
	[16]	0.828(23)	0.814(18)	0.802(18)	0.794(18)	0.795(30)

[a]From $\gamma = 1.156953(1)$ [19] and $\nu = 0.5875970(4)$ [20] via $\gamma = \nu(2-\eta)$ in (10).
[b]Given in [104] and compatible with 0.0365(10) [107] and $y_h = (5-\eta)/2 = 2.4820(2)$ in [108].
[c]From $y_t = 1/\nu = 1.3375(15)$ in [108], compatible with $\nu = 0.749(2)$ [107] and 0.750(2) [104].
[d]Computed from $\omega\nu = \Delta = 0.531(3)$ according to [109] and $\nu = 0.5875970(4)$ in [20].
[e]These are the results given as $\Delta_{S'} = 3 + \omega$ in Table 2 in [17].

resummation methods, we also show the outcome of applying our resummation procedure to the five-loop ε expansions, in comparison with the results given in [16] for the summation of the same series. It should be noted that we do not consider the renormalization in fixed dimension $D \in \{2, 3\}$, where the resummation problem is slightly different and has been approached, for example, with the *pseudo-ε expansion* [121,122] going back to Nickel (Ref. [19] in [6]).

The table furthermore includes a tiny selection of estimates obtained with other theoretical approaches (in particular Monte Carlo and the conformal bootstrap), which by no means can represent the vast literature on this subject. We merely tried to pick the most recent results of the highest apparent accuracy, in order to compare them against our field theoretic method.

Let us first state the following general observations:

(1) When we apply our resummation algorithm to the five-loop ε expansions, we obtain values for the critical exponents that are compatible with the resummation of [16]. This indicates that our resummation procedure is consistent with their method, though it differs from ours.[19]
(2) Our error estimates (at five loops) are smaller than those given in [16].
(3) The six-loop resummation results are consistent with the five-loop results (within the quoted errors), and in most cases the apparent errors of the six-loop results are significantly reduced compared to five loops.
(4) Overall the agreement of the six-loop resummation with predictions from other theoretical approaches is very good, in particular for η.

The largest apparent discrepancies between our six-loop resummation and other estimates occur for ω at $n = 0$ and the exponent ν when $n \geq 1$. In fact, the trend that renormalization-group-based predictions for ν tend to be lower than results from statistical approaches has been observed long ago. Our six-loop results narrow this gap only slightly, but due to the large error estimates in those cases we do not attach any significance to these differences yet. Once the seven-loop perturbative results become available, it will be interesting to revisit these cases.

We will now briefly discuss the universality classes one by one and, for completeness, show the full set of critical exponents as obtained via the scaling relations (10) from our resummation results for η and ν. However, these derived exponents might be determined more accurately via direct resummations of the individual series, as in [16], or other resummation techniques.

Note that we resum the ε expansions as explained in Sec. V, without enforcing any boundary values of exactly known critical exponents in two dimensions. The latter technique is often used to improve the resummation results for three dimensions [13,16,123]. However, the exact boundary values are not known in all cases, and it seems difficult to quantify the effect of this procedure on the error estimates. We therefore do not enforce any two-dimensional boundary values; instead, we test our method in Sec. VII by comparing our resummation results in two dimensions with exact predictions.

[19]Our method from Sec. V is an implementation of the ideas lined out in [13]. In [16], however, the authors abandoned the parameter λ from (30) and in its stead introduced a further parameter r via a transformation $f(\varepsilon) \mapsto (1 + r\varepsilon)f(\varepsilon)$.

A. Self-avoiding walks ($n=0$)

Over the last decade, successive improvements of Monte Carlo methods significantly diminished the uncertainty of critical exponents [19,20,124,125]. The latest and most accurate estimates are $\gamma = 1.156953(1)$ [19] and $\nu = 0.5875970(4)$ [20]. In contrast, the value $\omega\nu = \Delta = 0.531(3)$, computed long ago in [109] and confirmed by the very recent result 0.528(8) of [20], remains the most precise determination of the correction to scaling. In conclusion, we derive

$$\eta = 2 - \frac{\gamma}{\nu} = 0.031043(3) \quad \text{and} \quad \omega = \frac{\Delta}{\nu} = 0.904(5). \tag{37}$$

Applying the resummation procedure described in Sec. V to the six-loop ε expansions of η, ν and ω (Tables VIII–X) yields

$$\eta = 0.0310(7), \quad \nu = 0.5874(3) \quad \text{and} \quad \omega = 0.841(13). \tag{38}$$

The values of η and ν are in good agreement with (37), but the correction to scaling exponent ω differs by $\approx 7\%$. Note that our error estimate for ω increases from five to six loops, which hints towards a badly convergent situation.

For completeness, we compute the other critical exponents via the scaling relations (10) from (38):

$$\alpha = 0.2378(9), \quad \beta = 0.3028(4), \quad \gamma = 1.1566(10), \quad \delta = 4.820(4). \tag{39}$$

B. Ising universality class ($n=1$)

Experimental measurements in Ising systems, as discussed for example in [115,126,127], have rather larger uncertainties. Theoretical predictions are more accurate, like the Monte Carlo simulations [128] with

$$\eta = 0.03627(10), \quad \nu = 0.63002(10), \quad \omega = 0.832(6). \tag{40}$$

The most accurate values were obtained with the conformal bootstrap [18,106]:

$$\eta = 0.036298(2), \quad \nu = 0.629971(4), \quad \omega = 0.830(2). \tag{41}$$

Our resummations for η, ν and ω and the other exponents derived via (10) are

$$\eta = 0.0362(6), \quad \nu = 0.6292(5), \quad \omega = 0.820(7), \quad \alpha = 0.112(2), \quad \beta = 0.3260(5), \quad \gamma = 1.2356(14), \quad \delta = 4.790(4). \tag{42}$$

C. XY universality class ($n=2$)

Famous for the very precise measurement $\alpha = -0.0127(3)$ in the microgravity experiment at the λ transition of liquid helium [117], this universality class also describes planar Heisenberg magnets. Theoretical predictions from a combination of Monte Carlo simulations and high-temperature expansions in [103] are

$$\eta = 0.0381(2), \quad \nu = 0.6717(1), \quad \omega = 0.785(20), \quad \alpha = -0.0151(3), \quad \beta = 0.3486(1), \quad \gamma = 1.3178(2), \quad \delta = 4.780(1). \tag{43}$$

The conformal bootstrap [17] provides a correction to scaling exponent $\omega = \Delta_{S'} - 3 = 0.811(10)$. Resumming the six-loop ε expansions, we obtain

$$\eta = 0.0380(6), \quad \nu = 0.6690(10), \quad \omega = 0.804(3), \quad \alpha = -0.007(3), \quad \beta = 0.3472(7), \quad \gamma = 1.313(2), \quad \delta = 4.780(3), \tag{44}$$

where the values in the second and third row are calculated with the scaling relations (10). The accuracy for $\alpha = 2\text{–}3\nu$ is so small due to the vicinity of ν and $2/3$, and serves another motivation for the seven-loop calculation of the ε expansion.

D. Heisenberg universality class ($n=3$)

For experimental results, we refer to [129]. The most precise theoretical predictions stem from Monte Carlo simulations [104]:

$$\eta = 0.0378(3), \quad \nu = 0.7116(10); \tag{45}$$

Monte Carlo combined with high-temperature expansion [105]:

$$\eta = 0.0375(5), \quad \nu = 0.7112(5), \quad \alpha = -0.1336(15), \quad \beta = 0.3689(3), \quad \gamma = 1.3960(9), \quad \delta = 4.783(3); \tag{46}$$

and the correction to scaling exponent $\omega = \Delta_{S'} - 3 = 0.791(22)$ from the conformal bootstrap [17]. Our resummations yield

$$\eta = 0.0378(5), \quad \nu = 0.7059(20), \quad \omega = 0.795(7), \quad \alpha = -0.118(6), \quad \beta = 0.3663(12), \quad \gamma = 1.385(4), \quad \delta = 4.781(3). \tag{47}$$

E. The case $n=4$

The Monte Carlo results $\eta = 0.0360(3)$, $\nu = 0.750(2)$ from [104] and $\eta = 0.0365(10)$, $\nu = 0.749(2)$ given in

TABLE XII. Previous estimates for $D = 2$ dimensions from the five-loop ε expansion according to [13], our results for the resummation of the same series and also for six loops. The first row for the exponents η and ν shows the exact values for the Ising model (column $n = 1$) due to Onsager [132] and the conjectures of Nienhuis [133] in the cases $n = -1$ and $n = 0$. We also report theoretical expectations for the correction to scaling exponent ω.

		$n=-1$	$n=0$	$n=1$
η	[133]	0.15	0.208333…	0.25
	ε^6	0.130(17)	0.201(25)	0.237(27)
	ε^5	0.137(23)	0.215(35)	0.249(38)
	[13]		0.21(5)	0.26(5)
ν	[133]	0.625	0.75	1
	ε^6	0.6036(23)	0.741(4)	0.952(14)
	ε^5	0.6025(27)	0.747(20)	0.944(48)
	[13]		0.76(3)	0.99(4)
ω			$2^{[133,134]}$	$1.75^{[130]}$
	ε^6	1.95(28)	1.90(25)	1.71(9)
	ε^5	1.88(30)	1.83(25)	1.66(11)
	[13]		1.7(2)	1.6(2)

[107] are consistent with each other and also with the values $\eta = 0.0360(4)$, $\nu = 0.7477(8)$ obtained via $y_t = 1/\nu$ and $y_h = (5-\eta)/2$ from the results in [108]. The correction to scaling exponent is $\omega = \Delta_{S'} - 3 = 0.817(30)$ according to the conformal bootstrap [17].

Our resummation results and the scaling relations (10) lead to

$$\eta = 0.0366(4), \quad \nu = 0.7397(35), \quad \omega = 0.794(9),$$
$$\alpha = -0.219(11), \quad \beta = 0.383(2), \quad \gamma = 1.452(7),$$
$$\delta = 4.788(2). \tag{48}$$

VII. CRITICAL EXPONENTS IN TWO DIMENSIONS

In two dimensions, the resummation of critical exponents is known to be much less accurate, most likely due to nonanalyticities in the beta function at the critical point [130].[20] Indeed, our errors (determined automatically by the procedure from Sec. V D) reflect this expectation.

The results shown in Table XII are again compatible with the five-loop resummations from [13]. Furthermore, we can compare them with the following predictions:

$n = 1$.—The exact critical exponents $\eta = 1/4$ and $\nu = 1$ of the Ising model were computed by Onsager [132]. The convergence of our perturbative results seems slow, and in particular ν seems to stabilize at a value slightly lower than expected. This phenomenon of "anomalous apparent convergence" was already discussed in detail in [102] at the five-loop level and seems to persist at six loops.

The correction to scaling, however, is in good agreement with the prediction $\omega = 1.75$ from Eq. (21) in [130].

$n = 0$.—Our results are compatible with $\eta = 5/24$, $\nu = 3/4$ and $\omega = 2$ as already conjectured by Nienhuis [133], though ν again seems slightly too small and the uncertainty of ω is large. The value of ω has been subject to extensive debate [134], so increased accuracy from the seven-loop ε expansion would be particularly desirable here.

$n = -1$.—The value of η is roughly consistent with Nienhuis' $\eta = 3/20$, but for ν the prediction of $5/8$ is very far from our result (almost 10 times our error estimate).

VIII. SUMMARY AND OUTLOOK

After many years of work, new mathematical insights into the structure of Feynman integrals have matured into practically applicable techniques that overcome limitations of traditional approaches so far as to enable progress with the perturbative computation of renormalization group functions. Finally, after 25 years, we were thus able to improve on the five-loop results [14] of the $O(n)$-symmetric ϕ^4 model. We like to point out that the primitive graphs relevant to this computation have been essentially known for 30 years [42]. So the challenge was not in unknown transcendental numbers beyond zeta values, but the complexity introduced through subdivergences.

Our approach rests on a significantly improved understanding of the parametric representation of Feynman integrals [23,135], symbolic integration algorithms based on hyperlogarithms [24] and the Hopf algebra [136] of renormalization underlying the BPHZ scheme [25]. But also other techniques, like graphical functions and single-valued integration [46,137], can be used for this kind of calculations, as demonstrated by the impressive, independent work of Schnetz [26]. In fact, these methods are so powerful that even the seven-loop computation seems now not only feasible but is already underway [26]. Note that the contributions from seven-loop graphs without subdivergences were investigated numerically long ago [43,47] and are by now already known exactly [48].

We are optimistic that these tools will also have further applications. They should be particularly amenable to ϕ^3 theories, whose renormalization only very recently reached the four-loop level [123,138]. Fermions and gauge fields provide additional technical difficulties, but even in this very challenging domain, significant progress was achieved recently. Let us just mention the Gross-Neveu model [139] and the particularly impressive five-loop renormalization of QCD [140–142] and generalizations [143–145]. Those computations drew on yet another set of recently improved methods, e.g. [146–149].

[20] It seems, however, that the ε expansion yields much more accurate predictions for critical exponents in two dimensions (see Table XII) than the fixed dimension approach [131].

It is our hope that explicit longer perturbation series, like the ones presented here, will lead to an improved understanding of how they approach their asymptotic behavior and provide a sufficiently robust and precise testing ground to evaluate and compare the myriad of resummation methods that have been proposed over time, which usually make various unproven assumptions. Such an analysis is an important task in order to turn a finite number of perturbative coefficients reliably into very precise estimates for physical quantities and necessary to harvest the predictive power of increasingly high-order perturbation series. Ultimately, we hope that the deep theory of resurgence and transseries [150,151], in combination with the structure of Dyson-Schwinger equations [152], will provide superior tools for this task; but so far, its explicit practical lessons seem to restrict to the well-known insight that the analytic continuation of the Borel transform should be tailored to have the expected branch cuts [153].

As an application, we resummed the six-loop ε expansions for the critical exponents in three dimensions and found that, in many cases, the resulting reduction of their error estimates renders the renormalization group method again competitive in comparison with recently advanced bootstrap and Monte Carlo techniques. We expect that the seven-loop renormalization will provide critical exponents with even higher accuracies and allow for a more stringent analysis of the compatibility of these very different methods. This is an important task in order to check various assumptions that might be inherent to a particular approach. For example, recent bootstrap results assume that the $O(n)$ models are realized at a "kink" on the boundary of the domain of allowed operator dimensions [17,106].

ACKNOWLEDGMENTS

Both authors are indebted to Kostja Chetyrkin for hospitality at Karlsruhe Institute of Technology (KIT) in 2014, where this collaboration was started, and for encouraging us to undertake this six-loop project. We furthermore thank Oliver Schnetz for early access to the results of his independent computation, which reassured us on the correctness of our own calculations. The second author is also very grateful for an invitation to Friedrich-Alexander-Universität Erlangen-Nürnberg and very kind hospitality during this visit. Dmitrii Batkovich provided valuable checks of many six-loop integrals using the integration by parts (IBP)/infrared rearrangement (IRR)/R* method [50,62]. Also we thank John Gracey for reminding us of the large n-expansion results [55,56] for the β function and for discussions on the resummation of critical exponents. In particular the second author is grateful for hospitality at the University of Liverpool. David Broadhurst very kindly provided us with a copy of his notes [57], where he computed the minimal subtraction (MS)-renormalized five-loop propagator with extreme economy. The finite parts of these integrals form a subset of the six-loop counterterms and provided a valuable check of our results. Furthermore, we are grateful for Mikhail Nalimov's kind and helpful correspondence regarding the work [81,82] on the asymptotic expansions in dimensional regularization. Farrukh Chishtie and Tom Steele very kindly explained to us their work [73] on asymptotic Padé approximants and investigated the origin of the huge deviations of the six-loop predictions for γ_{m^2} at $n = 5$ (see footnote 7). We are also grateful to Andrey Kataev for fruitful discussions. In this manuscript, we incorporated several suggestions by John, David, Kostja, Mikhail, Oliver and an anonymous referee, who kindly read and commented on earlier drafts. We thank Simon Liebing for the precise translation of the title of [64]. Also we are grateful to Marc Bellon for discussions on the application of trans-series and resurgence to perturbative quantum field theory and hospitality at Laboratoire de Physique Théorique et Hautes Energies (LPTHE) Paris. Further thanks go to Christopher Beem for an illuminating explanation of the conformal bootstrap program. The work of the first author was supported by Russian Foundation for Basic Research (RFBR) Grant No. 17-02-00872-a. The second author's work on this project was supported by the Erwin Schrödinger International Institute for Mathematics and Physics (ESI) Vienna through the workshop "The interrelation between mathematical physics, number theory and noncommutative geometry" and the Mainz Institute for Theoretical Physics (MITP) program "Amplitudes: Practical and Theoretical Developments." He thanks both institutions for their hospitality during these inspiring meetings. This project was started while the second author was at the Institut des Hautes Études Scientifiques (IHÉS) with support from the European Research Council (ERC) Grant No. 257638 via the Centre national de la recherche scientifique (CNRS). The first author is grateful to All Souls College and the Mathematical Institute of the University of Oxford for hospitality and support during a visit in 2016. The calculations of the Z factors and the resummations of the critical exponents were performed on computers of the mathematical institutes of the Humboldt-Universität zu Berlin, the University of Oxford and the Resource Center "Computer Center of Saint Petersburg University." Figures of Feynman graphs in this article were created with JaxoDraw [154] and Axodraw [155].

APPENDIX A: DESCRIPTION OF ANCILLARY FILES

This article is accompanied by a comprehensive data set in the form of human readable text files. We provide these in two formats that are compatible with popular computer algebra software: Maple [156] (files ending with `.mpl`) and *Mathematica* [157] (files ending on `.m`). Concretely, these include

(i) ε expansions of the renormalization group functions and critical exponents,
(ii) individual counterterms (Z-factor contributions), symmetry and $O(n)$ factors of all ≤ 6 loop ϕ^4 graphs and

(iii) ε expansions of the massless propagators that we computed to obtain those.

Below we explain in detail the content and format of these files (referring only to the MAPLE files, since the *Mathematica* versions are built in complete analogy).

In addition, the Supplemental Material [158] (`resummation.pdf`) provides detailed information on our resummations. Namely, for each exponent $f \in \{\eta, \nu^{-1}, \omega\}$, dimension $D \in \{2, 3\}$ and the corresponding values of n considered in Tables XI and XII, it lists the parameters (b, λ, q) with least apparent error (36) together with plots like in Figs. 3 and 4, showing the nearby dependence on b and λ, and including the distribution of resummation results as in Fig. 6.

1. RG functions and critical exponents

Our six-loop expansions of the renormalization group functions β, γ_ϕ and γ_{m^2} defined in (4) and (5) are provided in the Supplemental Material [158], `expanded.mpl`, (in the MS scheme). It also contains the expansion of the critical coupling $g_\star(\varepsilon)$ from (6) and the resulting expansions for the universal critical exponents η, ν^{-1} and ω defined in (7) and (8), plus the critical exponents α, β, γ and δ computed via the scaling relations (10).

Each expansion is given symbolically with full n dependence, followed by numeric evaluations for $n \in \{0, 1, 2, 3, 4\}$ like in the tables in Secs. IV and V.

2. Counterterms of individual graphs

We computed the Z factors defined in (2) via their expansions (11) in counterterms. For each $i \in \{1, 2, 4\}$, the Supplemental Material [158] (`Z.mpl`) contains a list of graphs contributing to Z_i, similar to the table in Appendix A in [21] for Z_2. Each entry is of the form

$$\mathtt{Z}i[\ell, j] := [\mathrm{NI}(G), \mathrm{Sym}(G), \mathcal{C}_G, z_G]$$

and indexed by the loop number ℓ and an integer j. A graph G is specified by its Nickel index $\mathrm{NI}(G)$ as defined in Sec. II in [40]; see also [49]. This is an intuitive notation for an adjacency list with respect to a certain labeling of the vertices, illustrated in Fig. 8. Note that we consider graphs without fixed external labels ("non-leg-fixed" in the terminology of [69]); i.e. the symmetry factor is $\mathrm{Sym}(G) = (E_G)!/\mathrm{Aut}(G)$, where $E_G \in \{2, 4\}$ denotes the number of external legs and the automorphisms are allowed to permute them. Furthermore, the list contains the $O(n)$ group factor $\mathcal{C}_G$ from (15) and the actual counterterm contribution z_G, which, according to (11), equals $\partial_{p^2}\mathcal{KR}'G$ for Z_2 and $\mathcal{KR}'G$ for Z_4. The counterterm Z_1 is expressed as a linear combination of a subset of graphs contributing to Z_4, as explained in Sec. III.

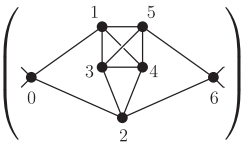

FIG. 8. The graph with Nickel index `ee12|345|346|45|5|6|ee|`, showing the vertex order corresponding to this labeling. This graph gives contributions to Z_1 and Z_4.

For example, the entry $Z4[6, 458]$ in `Z.mpl` corresponds to the graph G depicted in Fig. 8 with $\mathrm{NI}(G) =$ `ee12|345|346|45|5|6|ee|`. After minimal subtraction of subdivergences in the G scheme (A2), its pole part is

$$\mathcal{KR}'\left(\quad\right) = -\frac{\zeta_3}{3\varepsilon^4} + \left(\frac{5}{3}\zeta_3 + \frac{\pi^4}{180}\right)\frac{1}{\varepsilon^3} - \left(\frac{9}{2}\zeta_3 + \frac{7\pi^4}{360} - \frac{23}{6}\zeta_5\right)\frac{1}{\varepsilon^2} + \left(\frac{9}{2}\zeta_3 + \frac{7\pi^4}{360} - \frac{161}{30}\zeta_5 + \frac{7}{10}\zeta_3^2 - \frac{2\pi^6}{945}\right)\frac{1}{\varepsilon}. \tag{A1}$$

Multiplied with the symmetry and group factors $\mathrm{Sym}(G) = 3/2$ and $\mathcal{C}_G = (5n+22)(3n^2+22n+56)/2187$, this gives a contribution to Z_4. The counterterm (A1) also contributes to Z_1, but with symmetry factor $-1/2$ and group factor $(n+2)^2(5n+22)/243$, as dictated by entry $Z1[6, 473]$ in `Z.mpl`. Note that these data can also be looked up in [40], where the graph is called 603-U7 and drawings of all relevant graphs are provided in Fig. 1 therein.

The full Z factor is obtained by summing $(-g)^\ell \mathrm{Sym}(G)\mathcal{C}_G z_G$ over all entries of the corresponding list. The Supplemental Material [158] (`rg.mpl`) demonstrates this computation and furthermore generates the expansions of RG functions and critical exponents from these Z factors (it outputs the contents of `expanded.mpl` mentioned earlier).

3. ε expansions of massless propagators

We obtained the counterterms from massless propagators, which are also called "p integrals" [58], via the intermediate use of the BPHZ-like *one-scale scheme* [25] as explained in detail in [22]. Since these p integrals might be valuable for other applications, we include our results for their ε expansions in the Supplemental Material [158] (`p_int_gi.mpl`), where $i \in \{2, 4\}$. In the case $i = 2$, we list all 1PI propagator graphs of ϕ^4 theory, whereas the p integrals given for $i = 4$ arose from nullifying some

external momenta and rerouting external legs of some subdivergences, according to [22,25], in order to make those subdivergences single scale. In particular, this means that the p integrals listed for $i = 4$ are usually not Feynman graphs of ϕ^4 theory, due to vertices of valency greater than four.

The ε expansions are given for external momentum squared $p^2 = 1$ in the G scheme [38]: each integration over a loop momentum $\vec{k}$ carries the measure

$$\frac{\Gamma^2(1-\varepsilon)\Gamma(1+\varepsilon)}{\Gamma(2-2\varepsilon)} \int \frac{\mathrm{d}^{4-2\varepsilon}\vec{k}}{\pi^{2-\varepsilon}}, \tag{A2}$$

which in particular normalizes the bubble $\mathrm{NI}\left(\text{-}\bigcirc\text{-}\right) = \texttt{e11|e|}$, which is the first entry $p\mathrm{Int}[1,1]$ in `p_int_4.mpl`, to be exactly $1/\varepsilon$. For example, the entry $p\mathrm{Int}[6,163]$ with Nickel index `e123|e24|35|66|56|6||` gives the ε expansion

$$\left[\quad\right]_{p^2=1} = \frac{147\zeta_7}{16\varepsilon^2} - \left(\frac{147}{16}\zeta_7 + \frac{27}{2}\zeta_3\zeta_5 + \frac{27}{10}\zeta_{3,5} - \frac{2063\pi^8}{504000}\right)\frac{1}{\varepsilon} + \mathcal{O}\left(\varepsilon^0\right). \tag{A3}$$

APPENDIX B: ESTIMATES FOR PRIMITIVE DIAGRAMS UP TO 11 LOOPS

In the discussion of the asymptotic behavior in Sec. IV B, we included the contributions of primitive (subdivergence-free) graphs to the β function with up to 11 loops in Fig. 1. These graphs had been enumerated in [47], but exact results are currently complete only up to seven loops [48]. The Feynman integral of such a primitive four-point graph G with ℓ loops (and $\ell+1$ vertices) has a simple pole $\mathcal{P}(G)/(\ell\varepsilon)$ and thus contributes $-(-g)^\ell\mathcal{P}(G)/\ell$ to Z_4 and Z_g. Taking the symmetry factors into account, the resulting contributions $\beta^{\mathrm{prim}}(g) = \sum_k \beta_k^{\mathrm{prim}}(-g)^k$ to the beta function defined in (4) are

$$\beta_{\ell+1}^{\mathrm{prim}} = 2 \times \sum_{\substack{\text{primitive } G,\\ \ell \text{ loops, 4legs}}} \frac{\mathcal{P}(G)}{|\mathrm{Aut}(G)|}. \tag{B1}$$

The residue $\mathcal{P}(G)$ is known as the *Feynman period* [159] and can be written in Schwinger parameters x_e [one for each edge $e \in E(G)$ of the graph] as

$$\mathcal{P}(G) = \int_0^\infty \mathrm{d}x_2 \cdots \int_0^\infty \mathrm{d}x_{E(G)} \frac{1}{\psi_G^2(x)|_{x_1=1}}. \tag{B2}$$

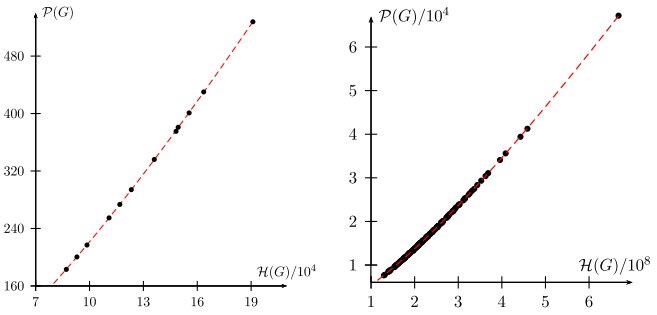

FIG. 9. The known Feynman periods $\mathcal{P}(G)$ at seven loops (left) and 11 loops (right) as a function of the Hepp bound $\mathcal{H}(G)$ from Definition 1. The plots also show the interpolating functions of the form (B5).

Here, the *Symanzik polynomial* ψ_G is given by a sum over spanning trees T of G:

$$\psi_G = \sum_{\substack{\text{spanning}\\ \text{tree} T}} \prod_{e\notin T} x_e. \tag{B3}$$

Beyond seven loops, not all Feynman periods are currently known [48]. Standard numerical techniques for the evaluation of (B2) are based on sector decomposition and Monte Carlo integration [68]. Unfortunately, these methods are not applicable in practice to graphs as complicated as the ϕ^4 graphs with 11 loops that we are facing here. However, we find that a decent numerical estimate for the integrals (B2) can be obtained from a rather simple graph invariant, constructed by approximating the Symanzik polynomial (B3) with its dominant (maximal) monomial.[21]

Definition 1.—The *Hepp bound* of a primitive ϕ^4 graph G is

$$\mathcal{H}(G) := \int_0^\infty \mathrm{d}x_2 \cdots \int_0^\infty \mathrm{d}x_{E(G)} \frac{1}{(\max_T \prod_{e\notin T} x_e)^2|_{x_1=1}} \in \mathbb{Q}. \tag{B4}$$

Note that $\mathcal{H}(G) \geq \mathcal{P}(G)$ is indeed an upper bound. It is much easier to compute than the actual period (B2); in particular, it is just a rational number and the calculation of the Hepp bounds for all primitive graphs with up to 11 loops is possible without much difficulty. The Hepp bound has many more interesting properties and will be explored in detail in a paper by the second author [160].

What is relevant for our purposes here is that, surprisingly, these easily obtainable numbers correlate strongly with the complicated Feynman period. For example, Fig. 9 shows the period $\mathcal{P}(G)$ as a function of the Hepp bound

[21]The integration domain can be subdivided into *Hepp sectors* $\{x\colon x_{\sigma(1)} < \cdots < x_{\sigma(E(G))}\}$, which are indexed by a permutation σ of the edges $E(G)$. Inside each Hepp sector, a particular monomial of ψ_G dominates all other monomials.

TABLE XIII. The upper part shows the counts of completed primitive ϕ^4 graphs and the estimates for the primitive contributions $\beta^{\text{prim}}_{\ell+1}$ to the beta function of the ϕ^4 model ($n=1$) at ℓ-loop order obtained with the Hepp bounds (B4). The lower part of the table shows the fitting parameters used in the approximation (B5).

Loop order ℓ	6	7	8	9	10	11
Completions	5	14	49	227	1354	9722
$\beta^{\text{prim}}_{\ell+1}$ estimate	2.41×10^4	3.71×10^5	6.06×10^6	1.05×10^8	1.89×10^9	3.57×10^{10}
$\beta^{\text{prim}}_{\ell+1}/\bar{\beta}^{\text{MS}}_{\ell+1}$	21.8%	26.2%	31.6%	37.6%	44.3%	51.5%
a_ℓ	$9.78/10^5$	$2.44/10^5$	$5.22/10^6$	$1.16/10^6$	$2.34/10^7$	$5.11/10^8$
b_ℓ	1.419	1.395	1.389	1.382	1.382	1.378
c_ℓ	$2.93/10^6$	$3.48/10^7$	$4.98/10^8$	$6.87/10^9$	$1.04/10^9$	$1.46/10^{10}$

$\mathcal{H}(G)$ at seven loops, where all periods are known exactly due to [48].

This relationship between $\mathcal{P}(G)$ and $\mathcal{H}(G)$ is well approximated by a power law and even better when we allow for one further parameter as in

$$\mathcal{P}(G)\approx f_\ell(\mathcal{H}(G)),\quad \text{where } f_\ell(h):=a_\ell h^{b_\ell}(1-hc_\ell). \tag{B5}$$

We fit the parameters a_ℓ, b_ℓ and c_ℓ to the known periods at loop order ℓ. The resulting coefficients are given in Table XIII and the plots of f_ℓ are shown in Fig. 9 for $\ell=7$ and $\ell=11$ loops. In all cases, the approximation by the very simple fit curves (B5) reproduces the known periods within 2% accuracy.[22] We note though that, with growing loop number, only very few periods are known exactly, as current integration techniques only apply to graphs with certain special combinatorial structures [48]. Our fits are thus biased—however, for the purpose of our discussion here, we expect this systematic error to be negligible.

To estimate the primitive contributions $\beta^{\text{prim}}_{\ell+1}$ to $\beta^{\text{MS}}_{\ell+1}$ at loop order ℓ, we substitute $f_\ell(\mathcal{H}(G))$ for $\mathcal{P}(G)$ in (B1). The calculation can be economized due to the fact that primitive graphs G with the same completion F (the completion is the 4-regular graph obtained by adding a vertex v and connecting it to the external legs, such that $G=F\backslash v$) have equal periods [47] and Hepp bounds. Therefore, $\mathcal{H}(F):=\mathcal{H}(F\backslash v)$ is independent of the choice of the vertex v. Table XIII summarizes the number of (isomorphism classes of) such completions, which were given also in Table 1 in [47]. We used NAUTY [161] to generate these graphs and to count their automorphisms.

Using the orbit-stabilizer theorem, $|\text{Aut}(F\backslash v)| = |\text{Stab}_{\text{Aut}(F)}(v)| = |\text{Aut}(F)|/|\text{Aut}(F)\cdot v|$, we can express the primitive contributions (B1) as a sum over the completed graphs as[23]

$$\beta^{\text{prim}}_{\ell+1}(n)\approx 2\cdot 4!\cdot(\ell+2)\times\sum_{\substack{\text{primitive } F,\\ \ell \text{ loops, 4-reg}}}\frac{f_\ell(\mathcal{H}(F))}{|\text{Aut}(F)|}\cdot\frac{3\mathcal{C}_F}{n(n+2)}, \tag{B6}$$

where we also made the group factor $\mathcal{C}_F$ from (13) explicit, using (15). In Table XIII we show the results for $n=1$ and see, for example, that at 11 loops, the primitive contributions amount to 51.5% of the asymptotic prediction $\bar{\beta}^{\text{MS}}_{12}$ from (20). Based on a comparison in the seven-loop case, where we know β^{prim}_8 exactly, we expect our estimates for $\beta^{\text{prim}}_{\ell+1}$ to be accurate within 1‰.

[22] This is a bound on the error for an individual period $\mathcal{P}(G)$ as approximated by $f_\ell(\mathcal{H}(G))$. On average, the error is much smaller.

[23] The factor 4! accounts for the different labelings of the external legs of a decompletion, and the $\ell+2$ vertices $V(F)=\dot{\bigcup}_{\text{orbits}}\text{Aut}(F)\cdot v$ are partitioned into the orbits corresponding to inequivalent uncompletions $G=F\backslash v$.

[1] H. Kleinert and V. Schulte-Frohlinde, Critical Properties of φ^4-Theories, (World Scientific, Singapore, 2001).

[2] A. N. Vasil'ev, *Quantum Field Renormalization Group in Critical Behavior Theory and Stochastic Dynamics* (Chapman and Hall/CRC, London, 2004), originally published in Russian in 1998 by St. Petersburg Institute of Nuclear Physics Press; translated by Patricia A. de Forcrand-Millard.

[3] J. Zinn-Justin, *Quantum Field Theory and Critical Phenomena*, International Series of Monographs on Physics Vol. 113, 4th ed. (Clarendon Press, Oxford, 2002).

[4] K. G. Wilson and M. E. Fisher, Critical Exponents in 3.99 Dimensions, Phys. Rev. Lett. **28**, 240 (1972).

[5] J. C. Le Guillou and J. Zinn-Justin, Critical Exponents for the n-Vector Model in Three Dimensions from Field Theory, Phys. Rev. Lett. **39**, 95 (1977).

[6] J. C. Le Guillou and J. Zinn-Justin, Critical exponents from field theory, Phys. Rev. B **21**, 3976 (1980).

[7] G. A. Baker, B. G. Nickel, M. S. Green, and D. I. Meiron, Ising-Model Critical Indices in Three Dimensions from the Callan-Symanzik equation, Phys. Rev. Lett. **36**, 1351 (1976).

[8] E. Brézin, J. C. Le Guillou, J. Zinn-Justin, and B. G. Nickel, Higher order contributions to critical exponents, Phys. Lett. **44A**, 227 (1973).

[9] A. A. Vladimirov, D. I. Kazakov, and O. V. Tarasov, Calculation of critical exponents by quantum field theory methods, Zh. Eksp. Teor. Fiz. **77**, 1035 (1979) [Sov. Phys. JETP **50**, 521 (1979)].

[10] K. G. Chetyrkin, S. G. Gorishny, S. A. Larin, and F. V. Tkachov, Five-loop renormalization group calculations in the $g\varphi^4$ theory, Phys. Lett. **132B**, 351 (1983).

[11] K. G. Chetyrkin, A. L. Kataev, and F. V. Tkachov, Five-loop calculations in the $g\varphi^4$ model and the critical index η, Phys. Lett. **99B**, 147 (1981); Erratum, Phys. Lett. **101B**, 457(E) (1981).

[12] D. I. Kazakov, The method of uniqueness, a new powerful technique for multiloop calculations, Phys. Lett. **133B**, 406 (1983).

[13] J. C. Le Guillou and J. Zinn-Justin, Accurate critical exponents from the ϵ-expansion, J. Phys. (Paris), Lett. **46**, 137 (1985).

[14] H. Kleinert, J. Neu, V. Schulte-Frohlinde, K. G. Chetyrkin, and S. A. Larin, Five-loop renormalization group functions of $O(n)$-symmetric ϕ^4-theory and ϵ-expansions of critical exponents up to ϵ^5, Phys. Lett. B **272**, 39 (1991); Erratum, Phys. Lett. B **319**, 545(E) (1993).

[15] L. T. Adzhemyan and M. V. Kompaniets, Five-loop numerical evaluation of critical exponents of the ϕ^4 theory, J. Phys. Conf. Ser. **523**, 012049 (2014).

[16] R. Guida and J. Zinn-Justin, Critical exponents of the N-vector model, J. Phys. A **31**, 8103 (1998).

[17] A. C. Echeverri, B. von Harling, and M. Serone, The effective bootstrap, J. High Energy Phys. 09 (2016) 097.

[18] F. Kos, D. Poland, D. Simmons-Duffin, and A. Vichi, Precision islands in the Ising and $O(N)$ models, J. High Energy Phys. 08 (2016) 036.

[19] N. Clisby, Scale-free Monte Carlo method for calculating the critical exponent γ of self-avoiding walks, J. Phys. A **50**, 264003 (2017).

[20] N. Clisby and B. Dünweg, High-precision estimate of the hydrodynamic radius for self-avoiding walks, Phys. Rev. E **94**, 052102 (2016).

[21] D. V. Batkovich, K. G. Chetyrkin, and M. V. Kompaniets, Six loop analytical calculation of the field anomalous dimension and the critical exponent η in $O(n)$-symmetric φ^4 model, Nucl. Phys. **B906**, 147 (2016).

[22] M. V. Kompaniets and E. Panzer, Renormalization group functions of ϕ^4 theory in the MS-scheme to six loops, Proc. Sci. LL2016 (**2016**) 038.

[23] F. C. S. Brown, The massless higher-loop two-point function, Commun. Math. Phys. **287**, 925 (2009).

[24] E. Panzer, Algorithms for the symbolic integration of hyperlogarithms with applications to Feynman integrals, Comput. Phys. Commun. **188**, 148 (2015).

[25] F. C. S. Brown and D. Kreimer, Angles, scales and parametric renormalization, Lett. Math. Phys. **103**, 933 (2013).

[26] O. Schnetz, Numbers and functions in quantum field theory, arXiv:1606.08598.

[27] R. Shrock, Question of an ultraviolet zero of the beta function of the $\lambda(\vec{\phi}^2)_4^2$ theory, Phys. Rev. D **90**, 065023 (2014).

[28] R. Shrock, Study of the six-loop beta function of the $\lambda\varphi_4^4$ theory, Phys. Rev. D **94**, 125026 (2016).

[29] H. Kleinert and V. Schulte-Frohlinde, Exact five-loop renormalization group functions of ϕ^4-theory with $O(N)$-symmetric and cubic interactions. critical exponents up to ϵ^5, Phys. Lett. B **342**, 284 (1995).

[30] A. I. Mudrov and K. B. Varnashev, Modified Borel summation of divergent series and critical-exponent estimates for an N-vector cubic model in three dimensions from five-loop ϵ expansions, Phys. Rev. E **58**, 5371 (1998).

[31] P. Calabrese, P. Parruccini, and A. I. Sokolov, Chiral phase transitions: Focus driven critical behavior in systems with planar and vector ordering, Phys. Rev. B **66**, 180403 (2002).

[32] G. A. Kalagov, M. V. Kompaniets, and M. Y. Nalimov, Renormalization-group investigation of a superconducting $U(r)$-phase transition using five loops calculations, Nucl. Phys. **B905**, 16 (2016).

[33] G. 't Hooft and M. Veltman, Regularization and renormalization of gauge fields, Nucl. Phys. **B44**, 189 (1972).

[34] J. C. Collins, Structure of counterterms in dimensional regularization, Nucl. Phys. **B80**, 341 (1974).

[35] G. 't Hooft, Dimensional regularization and the renormalization group, Nucl. Phys. **B61**, 455 (1973).

[36] N. N. Bogoliubov and O. S. Parasiuk, Über die Multiplikation der Kausalfunktionen in der Quantentheorie der Felder (On the multiplication of the causal function in the quantum theory of fields), Acta Math. **97**, 227 (1957).

[37] N. N. Bogoliubov and D. V. Shirkov, *Introduction to the Theory of Quantized Fields*, Interscience Monographs in Physics and Astronomy Vol. 3 (Interscience, New York, 1959), translated from Russian by G. M. Volkoff.

[38] K. G. Chetyrkin, A. L. Kataev, and F. V. Tkachov, New approach to evaluation of multiloop Feynman integrals: The Gegenbauer polynomial x-space technique, Nucl. Phys. **B174**, 345 (1980).

[39] A. A. Vladimirov, Methods of calculating many-loop diagrams and renormalization-group analysis of the φ^4 theory, Theor. Math. Phys. **36**, 732 (1978).

[40] B. G. Nickel, D. I. Meiron, and G. A. Baker, report, University of Guelph, available at http://users.physik.fu-berlin.de/~kleinert/nickel/.

[41] M. Borinsky, Renormalized asymptotic enumeration of Feynman diagrams, arXiv:1703.00840.

[42] D. J. Broadhurst, Technical Report No. OUT-4102-18, Open University, Milton Keynes, 1985.

[43] D. J. Broadhurst and D. Kreimer, Knots and numbers in ϕ^4 theory to 7 loops and beyond7, Int. J. Mod. Phys. C **06**, 519 (1995).
[44] E. Panzer, On the analytic computation of massless propagators in dimensional regularization, Nucl. Phys. **B874**, 567 (2013).
[45] O. Schnetz, Calculation of the φ^4 6-loop non-zeta transcendental, arXiv:hep-th/9912149.
[46] O. Schnetz, Graphical functions and single-valued multiple polylogarithms, Commun. Num. Theor. Phys. **8**, 589 (2014).
[47] O. Schnetz, Quantum periods: A census of ϕ^4-transcendentals, Commun. Num. Theor. Phys. **4**, 1 (2010).
[48] E. Panzer and O. Schnetz, The Galois coaction on ϕ^4 periods, arXiv:1603.04289.
[49] D. Batkovich, Y. Kirienko, M. Kompaniets, and S. Novikov, GraphState—A tool for graph identification and labelling, arXiv:1409.8227, program repository: https://bitbucket.org/mkompan/graph_state/downloads.
[50] D. V. Batkovich and M. V. Kompaniets, Toolbox for multiloop Feynman diagrams calculations using R^* operation, J. Phys. Conf. Ser. **608**, 012068 (2015).
[51] D. J. Broadhurst, Exploiting the 1,440-fold symmetry of the master two-loop diagram, Z. Phys. C **32**, 249 (1986).
[52] A. N. Vasil'ev, Y. M. Pis'mak, and Y. R. Honkonen, $1/n$ expansion: Calculation of the exponents η and ν in the order $1/n^2$ for arbitrary number of dimensions, Theor. Math. Phys. **47**, 465 (1981).
[53] A. N. Vasil'ev, Y. M. Pis'mak, and Y. R. Honkonen, Simple method of calculating the critical indices in the $1/n$ expansion, Theor. Math. Phys. **46**, 104 (1981).
[54] A. N. Vasil'ev, Y. M. Pis'mak, and Y. R. Honkonen, $1/n$ expansion: Calculation of the exponent ν in the order $1/n^3$ by the conformal bootstrap method, Theor. Math. Phys. **50**, 127 (1982).
[55] D. J. Broadhurst, J. A. Gracey, and D. Kreimer, Beyond the triangle and uniqueness relations: Non-zeta counterterms at large N from positive knots, Z. Phys. C **75**, 559 (1997).
[56] J. A. Gracey, Progress with large N_f β-functions, Nucl. Instrum. Methods Phys. Res., Sect. A **389**, 361 (1997).
[57] D. J. Broadhurst (unpublished).
[58] K. G. Chetyrkin and F. V. Tkachov, Integration by parts: The algorithm to calculate β-functions in 4 loops, Nucl. Phys. **B192**, 159 (1981).
[59] P. A. Baikov and K. G. Chetyrkin, Four loop massless propagators: An algebraic evaluation of all master integrals, Nucl. Phys. **B837**, 186 (2010).
[60] R. N. Lee, A. V. Smirnov, and V. A. Smirnov, Master integrals for four-loop massless propagators up to weight twelve, Nucl. Phys. **B856**, 95 (2012).
[61] A. V. Smirnov and M. Tentyukov, Four-loop massless propagators: A numerical evaluation of all master integrals, Nucl. Phys. **B837**, 40 (2010).
[62] D. V. Batkovich and M. V. Kompaniets (to be published).
[63] K. G. Chetyrkin, Combinatorics of R-, R^{-1}-, and R^*-operations and asymptotic expansions of feynman integrals in the limit of large momenta and masses, arXiv:1701.08627.
[64] K. G. Chetyrkin, S. G. Gorishny, S. A. Larin, and F. V. Tkachov, Institute for Nuclear Research Report No. INR P-0453, Moscow, in Russian, 1986.
[65] K. G. Chetyrkin and V. A. Smirnov, R^*-operation corrected, Phys. Lett. **144B**, 419 (1984).
[66] K. G. Chetyrkin and F. V. Tkachov, Infrared R-operation and ultraviolet counterterms in the MS-scheme, Phys. Lett. **114B**, 340 (1982)4.
[67] E. Panzer, Ph. D. thesis, Humboldt-Universität zu Berlin, 2014, arXiv:1506.07243.
[68] T. Binoth and G. Heinrich, An automatized algorithm to compute infrared divergent multiloop integrals, Nucl. Phys. **B585**, 741 (2000).
[69] M. Borinsky, Feynman graph generation and calculations in the Hopf algebra of Feynman graphs, Comput. Phys. Commun. **185**, 3317 (2014);Programs also available at https://github.com/michibo/feyncop.
[70] J. A. M. Vermaseren, New features of FORM, arXiv:math-ph/0010025.
[71] M. V. Kompaniets, Prediction of the higher-order terms based on Borel resummation with conformal mapping, J. Phys. Conf. Ser. **762**, 012075 (2016).
[72] J. Ellis, M. Karliner, and M. A. Samuel, A prediction for the 4-loop β function in QCD, Phys. Lett. B **400**, 176 (1997).
[73] F. Chishtie, V. Elias, and T. G. Steele, Asymptotic Padé-approximant predictions for renormalization-group functions of massive ϕ^4 scalar field theory, Phys. Lett. B **446**, 267 (1999).
[74] E. Brézin, J. C. Le Guillou, and J. Zinn-Justin, Perturbation theory at large order. I. The φ^{2N} interaction, Phys. Rev. D **15**, 1544 (1977).
[75] L. N. Lipatov, Divergence of the perturbation-theory series and the quasi-classical theory, Zh. Eksp. Teor. Fiz. **72**, 411 (1977) [Sov. Phys. JETP **45**, 216 (1977)].
[76] A. J. McKane, D. J. Wallace, and O. F. de Alcantara Bonfim, Non-perturbative renormalisation using dimensional regularisation: Applications to the ϵ expansion, J. Phys. A **17**, 1861 (1984).
[77] A. J. McKane and D. J. Wallace, Instanton calculations using dimensional regularisation, J. Phys. A **11**, 2285 (1978).
[78] F. M. Dittes, Y. A. Kubyshin, and O. V. Tarasov, Four-loop approximation in the ϕ^4 model, Theor. Math. Phys. **37**, 879 (1978).
[79] D. I. Kazakov, O. V. Tarasov, and D. V. Širkov, Analytic continuation of the results of perturbation theory for the model $g\phi^4$ to the region $g \gtrsim 1$, Theor. Math. Phys. **38**, 9 (1979).
[80] Y. A. Kubyshin, Corrections to the asymptotic expressions for the higher orders of perturbation theory, Theor. Math. Phys. **57**, 1196 (1983).
[81] M. V. Komarova and M. Y. Nalimov, Large-order asymptotic terms in perturbation theory: The first $(4-\epsilon)$-expansion correction to renormalization constants in the $O(n)$-symmetric theory, Theor. Math. Phys. **143**, 664 (2005).
[82] M. V. Komarova and M. Y. Nalimov, Asymptotic behavior of renormalization constants in higher orders of the perturbation expansion for the $(4-\varepsilon)$-dimensionally regularized $O(n)$-symmetric ϕ^4 theory, Theor. Math. Phys. **126**, 339 (2001).

[83] D. A. Lobaskin and I. M. Suslov, Higher order corrections to the Lipatov asymptotics in the ϕ^4 theory, Zh. Eksp. Teor. Fiz. **99**, 268 (2004) [J. Exp. Theor. Phys. **99**, 234 (2004)].
[84] I. M. Suslov, Structure of higher order corrections to the Lipatov asymptotic form, J. Exp. Theor. Phys. **90**, 571 (2000).
[85] D. I. Kazakov and V. S. Popov, On the summation of divergent perturbation series in quantum mechanics and field theory, J. Exp. Theor. Phys. **95**, 581 (2002).
[86] D. I. Kazakov and V. S. Popov, Asymptotic behavior of the Gell-Mann-Low function in quantum field theory, JETP Lett. **77**, 453 (2003).
[87] P. V. Pobylitsa, Superfast convergence effect in large orders of the perturbative and ϵ expansions for the $O(N)$ symmetric ϕ^4 model, arXiv:0807.5136.
[88] M. Borinsky, Generating asymptotics for factorially divergent sequences, arXiv:1603.01236.
[89] E. Caliceti, M. Meyer-Hermann, P. Ribeca, A. Surzhykov, and U. D. Jentschura, From useful algorithms for slowly convergent series to physical predictions based on divergent perturbative expansions, Phys. Rep. **446**, 1 (2007).
[90] R. Seznec and J. Zinn-Justin, Summation of divergent series by order dependent mappings: Application to the anharmonic oscillator and critical exponents in field theory, J. Math. Phys. (N.Y.) **20**, 1398 (1979).
[91] J. Zinn-Justin, Summation of divergent series: Order-dependent mapping, Applied Numerical Mathematics **60**, 1454 (2010).
[92] H. Kleinert, Critical exponents from seven-loop strong-coupling φ^4 theory in three dimensions, Phys. Rev. D **60**, 085001 (1999).
[93] H. Kleinert, Converting divergent weak-coupling into exponentially fast convergent strong-coupling expansions, Electron. J. Theor. Phys. **8**, 15 (2011).
[94] H. Kleinert and V. Schulte-Frohlinde, Critical exponents from five-loop strong-coupling ϕ^4-theory in $4-\varepsilon$ dimensions, J. Phys. A **34**, 1037 (2001).
[95] V. I. Yukalov and E. P. Yukalova, Calculation of critical exponents by self-similar factor approximants, Eur. Phys. J. B **55**, 93 (2007).
[96] S. G. Gorishny, S. A. Larin, and F. V. Tkachov, ε-expansion for critical exponents: The $O(\varepsilon^5)$ approximation, Phys. Lett. **101A**, 120 (1984).
[97] J.-P. Eckmann, J. Magnen, and R. Sénéor, Decay properties and Borel summability for the Schwinger functions in $P(\Phi)_2$ theories, Commun. Math. Phys. **39**, 251 (1975).
[98] J. Magnen and R. Sénéor, Phase space cell expansion and Borel summability for the Euclidean φ^4_3 theory, Commun. Math. Phys. **56**, 237 (1977).
[99] H. Mera, T. G. Pedersen, and B. K. Nikolić, Nonperturbative Quantum Physics from Low-Order Perturbation Theory, Phys. Rev. Lett. **115**, 143001 (2015).
[100] W. A. A. Gaddah and I. S. Jwan, in *Proceedings of the 3rd National Conference of Basic Science 25–27/4/2009 Aljabal Algharbi University, Gharian, Libya* (2009), pp. 175–182.
[101] U. D. Jentschura and G. Soff, Improved conformal mapping of the Borel plane, J. Phys. A **34**, 1451 (2001).
[102] B. Delamotte, M. Dudka, Y. Holovatch, and D. Mouhanna, Relevance of the fixed dimension perturbative approach to frustrated magnets in two and three dimensions, Phys. Rev. B **82**, 104432 (2010).
[103] M. Campostrini, M. Hasenbusch, A. Pelissetto, and E. Vicari, Theoretical estimates of the critical exponents of the superfluid transition in ^{4}He by lattice methods, Phys. Rev. B **74**, 144506 (2006).
[104] M. Hasenbusch and E. Vicari, Anisotropic perturbations in three-dimensional $O(N)$-symmetric vector models, Phys. Rev. B **84**, 125136 (2011).
[105] M. Campostrini, M. Hasenbusch, A. Pelissetto, P. Rossi, and E. Vicari, Critical exponents and equation of state of the three-dimensional Heisenberg universality class, Phys. Rev. B **65**, 144520 (2002).
[106] S. El-Showk, M. F. Paulos, D. Poland, S. Rychkov, D. Simmons-Duffin, and A. Vichi, Solving the 3d Ising model with the conformal bootstrap II. c-minimization and precise critical exponents, J. Stat. Phys. **157**, 869 (2014).
[107] M. Hasenbusch, Eliminating leading corrections to scaling in the three-dimensional $O(N)$ symmetric ϕ^4 model: $N = 3$ and 4, J. Phys. A **34**, 8221 (2001).
[108] Y. Deng, Bulk and surface phase transitions in the three-dimensional $O(4)$ spin model, Phys. Rev. E **73**, 056116 (2006).
[109] P. Belohorec, Ph. D. thesis, University of Guelph, 1997; Advisor, B. G. Nickel, available at http://www.collectionscanada.gc.ca/obj/s4/f2/dsk3/ftp04/nq24397.pdf.
[110] P. M. Stevenson, Resolution of the renormalisation-scheme ambiguity in perturbative QCD, Phys. Lett. **100B**, 61 (1981).
[111] G. Grunberg, Renormalization group improved perturbative QCD, Phys. Lett. **95B**, 70 (1980); Erratum, Phys. Lett. **110B**, 501(E) (1982).
[112] J. M. Carmona, A. Pelissetto, and E. Vicari, N-component Ginzburg-Landau Hamiltonian with cubic anisotropy: A six-loop study, Phys. Rev. B **61**, 15136 (2000).
[113] A. Butti and F. P. Toldin, The critical equation of state of the three-dimensional $O(N)$ universality class: $N > 4$, Nucl. Phys. **B704**, 527 (2005).
[114] F. Jasch and H. Kleinert, Fast-convergent resummation algorithm and critical exponents of ϕ^4-theory in three dimensions, J. Math. Phys. (N.Y.) **42**, 52 (2001).
[115] A. Pelissetto and E. Vicari, Critical phenomena and renormalization-group theory, Phys. Rep. **368**, 549 (2002).
[116] P.-G. de Gennes, *Scaling Concepts in Polymer Physics* (Cornell University Press, London, 1979).
[117] J. A. Lipa, J. A. Nissen, D. A. Stricker, D. R. Swanson, and T. C. P. Chui, Specific heat of liquid helium in zero gravity very near the lambda point, Phys. Rev. B **68**, 174518 (2003).
[118] R. D. Pisarski and F. Wilczek, Remarks on the chiral phase transition in chromodynamics, Phys. Rev. D **29**, 338 (1984).
[119] S. A. Antonenko and A. I. Sokolov, Critical exponents for a three-dimensional $O(n)$-symmetric model with $n > 3$, Phys. Rev. E **51**, 1894 (1995).
[120] S. Holtmann and T. Schulze, Critical behavior and scaling functions of the three-dimensional $O(6)$ model, Phys. Rev. E **68**, 036111 (2003).
[121] M. A. Nikitina and A. I. Sokolov, Critical exponents in two dimensions and pseudo-ϵ expansion, Phys. Rev. E **89**, 042146 (2014).

[122] A. I. Sokolov and M. A. Nikitina, Fisher exponent from pseudo-ϵ expansion, Phys. Rev. E **90**, 012102 (2014).
[123] J. A. Gracey, Four loop renormalization of ϕ^3 theory in six dimensions, Phys. Rev. D **92**, 025012 (2015).
[124] N. Clisby, Accurate Estimate of the Critical Exponent ν for Self-Avoiding Walks via a Fast Implementation of the Pivot Algorithm, Phys. Rev. Lett. **104**, 055702 (2010).
[125] N. Clisby, R. Liang, and G. Slade, Self-avoiding walk enumeration via the lace expansion, J. Phys. A **40**, 10973 (2007).
[126] A. Lytle and D. T. Jacobs, Turbidity determination of the critical exponent η in the liquid-liquid mixture methanol and cyclohexane, J. Chem. Phys. **120**, 5709 (2004).
[127] J. V. Sengers and J. G. Shanks, Experimental critical-exponent values for fluids, J. Stat. Phys. **137**, 857 (2009).
[128] M. Hasenbusch, Finite size scaling study of lattice models in the three-dimensional Ising universality class, Phys. Rev. B **82**, 174433 (2010).
[129] N. Ghosh, S. Rößler, U. K. Rößler, K. Nenkov, S. Elizabeth, H. L. Bhat, K. Dörr, and K.-H. Müller, Heisenberg-like critical properties in ferromagnetic $Nd_{1-x}Pb_xMnO_3$ single crystals, J. Phys. Condens. Matter **18**, 557 (2006).
[130] P. Calabrese, M. Caselle, A. Celi, A. Pelissetto, and E. Vicari, Non-analyticity of the Callan-Symanzik β-function of two-dimensional $O(N)$ models, J. Phys. A **33**, 8155 (2000).
[131] E. V. Orlov and A. I. Sokolov, Critical thermodynamics of two-dimensional systems in the five-loop renormalization-group approximation, Phys. Solid State **42**, 2151 (2000).
[132] L. Onsager, Crystal Statistics. I. A Two-Dimensional Model with an Order-Disorder Transition, Phys. Rev. **65**, 117 (1944).
[133] B. Nienhuis, Exact Critical Point and Critical Exponents of $O(n)$ Models in Two Dimensions, Phys. Rev. Lett. **49**, 1062 (1982).
[134] S. Caracciolo, A. J. Guttmann, I. Jensen, A. Pelissetto, A. N. Rogers, and A. D. Sokal, Correction-to-scaling exponents for two-dimensional self-avoiding walks, J. Stat. Phys. **120**, 1037 (2005).
[135] F. C. S. Brown, On the periods of some Feynman integrals, arXiv:0910.0114.
[136] A. Connes and D. Kreimer, Renormalization in quantum field theory and the Riemann-Hilbert problem I: The Hopf algebra structure of graphs and the main theorem, Commun. Math. Phys. **210**, 249 (2000).
[137] M. Golz, E. Panzer, and O. Schnetz, Graphical functions in parametric space, Lett. Math. Phys. **107**, 1177 (2017).
[138] J. A. Gracey, F_4 symmetric ϕ^3 theory at four loops, Phys. Rev. D **95**, 065030 (2017).
[139] J. A. Gracey, T. Luthe, and Y. Schröder, Four loop renormalization of the Gross-Neveu model, Phys. Rev. D **94**, 125028 (2016).
[140] P. A. Baikov, K. G. Chetyrkin, and J. H. Kühn, Five-Loop Running of the QCD Coupling Constant, Phys. Rev. Lett. **118**, 082002 (2017).
[141] T. Luthe, A. Maier, P. Marquard, and Y. Schröder, Complete renormalization of QCD at five loops, J. High Energy Phys. 03 (2017) 020.
[142] B. Ruijl, T. Ueda, J. A. M. Vermaseren, and A. Vogt, Four-loop QCD propagators and vertices with one vanishing external momentum, J. High Energy Phys. 06 (2017) 040.
[143] P. A. Baikov, K. G. Chetyrkin, and J. H. Kühn, Five-loop fermion anomalous dimension for a general gauge group from four-loop massless propagators, J. High Energy Phys. 04 (2017) 119.
[144] F. Herzog, B. Ruijl, T. Ueda, J. A. M. Vermaseren, and A. Vogt, The five-loop beta function of Yang-Mills theory with fermions, J. High Energy Phys. 02 (2017) 090.
[145] T. Luthe, A. Maier, P. Marquard, and Y. Schröder, Five-loop quark mass and field anomalous dimensions for a general gauge group, J. High Energy Phys. 01 (2017) 081.
[146] P. A. Baikov, Explicit solutions of the multi-loop integral recurrence relations and its application, Nucl. Instrum. Methods Phys. Res., Sect. A **389**, 347 (1997).
[147] F. Herzog and B. Ruijl, The R^*-operation for Feynman graphs with generic numerators, J. High Energy Phys. 05 (2017) 037.
[148] T. Luthe and Y. Schröder, Five-loop massive tadpoles, Proc. Sci. LL2016 (**2016**) 074.
[149] B. Ruijl, T. Ueda, and J. A. M. Vermaseren, Forcer: A FORM program for 4-loop massless propagators, Proc. Sci. LL2016 (**2016**) 070.
[150] D. Dorigoni, An introduction to resurgence, trans-series and alien calculus, arXiv:1411.3585.
[151] G. V. Dunne and M. Ünsal, Resurgence and trans-series in quantum field theory: The $\mathbb{CP}^{N-1}$ model, J. High Energy Phys. 11 (2012) 170.
[152] M. P. Bellon and P. J. Clavier, A Schwinger-Dyson equation in the Borel plane: Singularities of the solution, Lett. Math. Phys. **105**, 795 (2015).
[153] A. Cherman, P. Koroteev, and M. Ünsal, Resurgence and holomorphy: From weak to strong coupling, J. Math. Phys. (N.Y.) **56**, 053505 (2015).
[154] D. Binosi and L. Theußl, JaxoDraw: A graphical user interface for drawing Feynman diagrams, Comput. Phys. Commun. **161**, 76 (2004).
[155] J. A. M. Vermaseren, Axodraw, Comput. Phys. Commun. **83**, 45 (1994).
[156] Maplesoft, a division of Waterloo Maple Inc., "Maple 16".
[157] Wolfram Research, Inc., Mathematica 11.0, 2016.
[158] See Supplemental Material at http://link.aps.org/supplemental/10.1103/PhysRevD.96.036016 for files containing the renormalization group functions, counterterms, ϵ-expansions and critical exponents (as described in detail in Appendix A).
[159] S. Bloch, H. Esnault, and D. Kreimer, On motives associated to graph polynomials, Commun. Math. Phys. **267**, 181 (2006).
[160] E. Panzer (to be published).
[161] B. D. McKay and A. Piperno, Practical graph isomorphism, II, J. Symb. Comput. **60**, 94 (2014); program website: http://pallini.di.uniroma1.it/.